NASA TECHNICAL NOTE

SEASONAL AND GEOGRAPHIC VARIATION OF ATMOSPHERIC OZONE, DERIVED FROM NIMBUS 3

by C. Prabhakara, B. J. Conrath, L. J. Allison, and J. Steranka

Goddard Space Flight Center
Greenbelt, Md.   20771

0132937

1. Report No. NASA TN D-6443	2. Government Accession No.	3. Recipient's Catalog No.
4. Title and Subtitle Seasonal and Geographic Variation of Atmospheric Ozone, Derived from Nimbus 3		5. Report Date August 1971
		6. Performing Organization Code
7. Author(s) C. Prabhakara, B. J. Conrath, L. J. Allison, J. Steranka		8. Performing Organization Report No. G-1027
9. Performing Organization Name and Address Goddard Space Flight Center Greenbelt, Md. 20771		10. Work Unit No.
		11. Contract or Grant No.
12. Sponsoring Agency Name and Address National Aeronautics and Space Administration Washington, D.C. 20546		13. Type of Report and Period Covered Technical Note
		14. Sponsoring Agency Code

15. Supplementary Notes

16. Abstract

Nimbus 3 infrared interferometer spectrometer (IRIS) measurements of the intensities in the 9.6-μm region are used to derive the ozone content in the atmosphere between latitudes 80°N and 80°S.

The global distribution of total ozone was mapped for eight days in April and eight days in July 1969. These global maps of total ozone are compared with the upper-air constant-pressure maps to emphasize the meteorological significance of the ozone variations in time and space.

The total ozone has a minimum value of about 0.25 cm STP in the equatorial regions and increases markedly toward both poles. In the Arctic region, the total ozone in the springtime is well above 0.5 cm STP, while in summer it is about 0.4 cm STP.

An eight-day mean global map of total ozone for April 1969 clearly reveals the presence of climatological large-scale ozone systems in the atmosphere. Another such map, for July 1969, shows that these systems have weakened considerably in the northern hemisphere. Seasonal variability in the total ozone over the southern hemisphere is much less pronounced.

Close association between the total-ozone systems and tropospheric weather systems is shown for several cases. From this study, it is concluded that the atmospheric ozone, remotely sensed by satellites, can be used as a meteorological parameter to diagnose the present state of the atmosphere, and, thereby, aid weather prediction.

17. Key Words Suggested by Author Ozone 300-mb circulation	18. Distribution Statement Unclassified-Unlimited

19. Security Classif. (of this report) Unclassified	20. Security Classif. (of this page) Unclassified	21. No. of Pages 61	22. Price * 3.00

CONTENTS

SEASONAL AND GEOGRAPHIC VARIATION OF ATMOSPHERIC OZONE, DERIVED FROM NIMBUS 3

by
C. Prabhakara
B. J. Conrath
L. J. Allison
J. Steranka

Goddard Space Flight Center

INTRODUCTION

The meteorological significance of atmospheric ozone was recognized as early as 1927 by Dobson and his associates (Dobson et al., 1927). Since then, numerous studies have been made on this subject. (For a comprehensive review and bibliography, see Craig, 1950, Ramanathan, 1954, Paetzold and Regener, 1957, Griggs, 1966, Dütsch, 1969.) These investigations, in general, show that the surface low-pressure regions are associated with above average amounts of total ozone and the surface high-pressure regions are associated with below average amounts. The height of the tropopause and the temperatures in the upper tropopause and lower stratosphere show significant correlations with the total ozone (Meetham, 1937). More recent synoptic studies by Danielson (1968), Breiland (1969), and others have further clarified the significance of ozone variations in association with the above-mentioned parameters.

Normally, the total ozone is observed to be low in the tropical latitudes (approximately 0.25 cm STP) with small (approximately 5 percent) daily and seasonal variations. On the other hand, for middle and higher latitudes the ozone amounts observed are higher (approximately 0.35 cm STP) with correspondingly larger (approximately 10 percent) daily and seasonal variations.

The association of these seasonal, daily, and geographic variations of ozone with meteorological changes is a matter of great interest. However, as there are only a limited number of stations over the globe where total-ozone measurements are routinely made, there is no complete picture of the behavior of ozone on a global scale. Vertical soundings of ozone are made at an even smaller number of stations. (See Kohmyr and Sticksel, 1967 and Hering and Borden, 1965 and 1967 for collections of ozone soundings.) The Nimbus 3 satellite, which orbits the earth from 80°N to 80°S with an

1

infrared interferometer spectrometer (IRIS) on board, has greatly improved our ability to measure remotely the atmospheric ozone content. This remote sounding device will be discussed in this paper.

The IRIS instrument operated successfully from April 15 to July 22, 1969. In this report, a detailed study is presented of the global ozone distribution for two periods of eight days each in April and July of 1969. In Appendix A, the 50- and 10-mb global temperature distribution maps for April 25-29, 1969, are also presented and briefly discussed.

BACKGROUND

Photochemistry and Meteorology of Atmospheric Ozone

So that the interrelation of ozone systems with large-scale circulation can be better appreciated, the basic facts concerning the photochemical theory of atmospheric ozone will be discussed in this section. Solar ultraviolet radiation (<2420 Å), when absorbed by molecular oxygen present in the air, dissociates it into atomic oxygen. Some of the resulting atomic oxygen can combine on collision with molecular oxygen to form ozone. However, the ozone formed in this manner also strongly absorbs the solar near-UV radiation and, thereby, dissociates back to molecular and atomic oxygen. The formation and destruction of ozone reaches an equilibrium state and leaves only a small amount (a few parts per million) present at any time in the ambient air.

The scheme described above is based on the photochemical theory of atmospheric ozone first proposed by Chapman (1930). Since then, several additional reactions involving water vapor and hydrogen have been added to this basic scheme (Hampson, 1964, Hunt, 1966, and Leovy, 1969). Calculations by many investigators of the photochemically produced vertical distribution of ozone show, in general, a maximum concentration of ozone somewhere near the 25-km altitude. This concentration decreases at levels above 25 km because of lower atmospheric density, and in the denser layers below 25 km, it decreases rather rapidly with altitude as a consequence of exponential attenuation of solar UV by molecular oxygen and ozone. Furthermore, the photochemical calculations indicate that there will be more ozone in tropical latitudes than in high latitudes as a result of the longer oblique path of solar rays through the atmosphere to high latitudes. From the manner in which the ozone is produced, one can readily see that at high levels in the atmosphere, above about 30 km where the incident solar UV radiation is strong, photochemical equilibrium will be established quite rapidly. As one goes progressively to the lower layers, toward the tropopause, the time photochemical equilibrium takes to be established increases rapidly as the solar UV attenuates exponentially with depth. For this reason, if ozone is brought down to below 30 km, it can exist for days, or even months. However, this situation changes drastically below the tropopause, where other types of destruction become dominant. Because of tropospheric mixing, ozone comes into contact with the ground and is destroyed (Regener, 1957). Tropospheric aerosols

also contribute to ozone destruction (Junge, 1962). Thus, the lower stratosphere, where ozone can survive for a long time, is seen to be the region that favors its accumulation.

As a consequence, the photochemical theory cannot explain the temporal and spatial variations of ozone. Ozone is transported by eddy mixing, and winds play a dominant role in its transient behavior. As is well known (Newell, 1964), the circulations in the lower stratosphere are driven by the troposphere. The long waves of the troposphere can influence layers of the lower stratosphere (Peng, 1965). With this intimate association between the troposphere and stratosphere, it should be expected that changes of ozone in the lower stratosphere would reflect changes in the wind field in the upper troposphere.

The present study focuses attention particularly on the broad-scale, global distribution of ozone, derived from IRIS for several individual days, and its close association with tropospheric weather systems.

Brief Survey of Ozone Measuring Techniques

Atmospheric ozone is commonly determined from Dobson-spectrophotometer measurements of the intensity of UV, either directly incident from the sun or scattered from the zenith sky. Total-ozone content of the atmosphere is determined from the solar UV, attenuated by ozone absorption and molecular scattering, that reaches the instrument (Dobson, 1931). It is also possible to compute the vertical distribution of ozone by the Umkehr method whenever zenith-sky measurements are made at different angles of solar elevation (Gotz et al., 1934). The Dobson spectrophotometric measurements have allowed exploration of the behavior of atmospheric ozone as a function of latitude, but the complexity of the instrument and the calculations has limited the number of observing stations.

Several methods for measuring the vertical distribution of ozone with balloon- and rocket-borne instruments have been developed. Paetzold's method (1953) measures the variation with altitude of the solar UV intensity in selected spectral regions with a balloon-borne radiometer, and, thereby, permits the integrated ozone amount above the balloon altitude to be computed. The vertical distribution of ozone is obtained by differentiation. Krueger (1969) and Nagata et al. (1967) have developed ozone measuring methods based on similar radiometric measurements.

Regener (1964) developed an ozone sounder in which chemiluminescent dye reacts when oxidized with ozone. The luminescence is monitored to measure the in situ ozone concentration. Hilsenrath et al. (1969) and Randhawa (1967) have also developed ozone measuring techniques based on the chemiluminescence principle.

Brewer and Milford (1960) have developed a chemical ozone sounder based on the reaction

$$2KI + O_3 + H_2O \rightarrow O_2 + 2KOH + I_2.$$

This method also yields ozone concentration, in situ. Furthermore, since the electrochemical reactions can be followed quantitatively, this technique can be used as an absolute calibration of other methods. Komhyr (1965) has developed a carbon-iodine chemical sounder along similar lines.

Satellite-borne ultraviolet spectrometers have been used to sense the ozone distribution at high altitudes (Rawcliffe et al., 1963, and Iozenas et al., 1969), but they could not probe the atmosphere below about 20 mb. Recently a backscatter-ultraviolet spectrometer experiment, on board the Nimbus 4 satellite, has measured the vertical distribution and total amount of ozone quite accurately. *

Epstein et al. (1956) used the absorption and emission properties of ozone in the 9.6-μm region to obtain the vertical distribution of ozone. This ground-based method was not very successful (Dave et al., 1963) since tropospheric water vapor and aerosols severely affect the 9.6-μm O_3-band intensity measurements. However, when the earth is viewed from a space platform in the 9.6-μm region, these tropospheric effects do not pose a problem because they can be quantitatively eliminated in the method of inversion as shown by Prabhakara et al. (1970).

REMOTE SOUNDING METHOD

There is, on the average, about 0.35 cm STP of ozone per cm^2 on the earth, concentrated mostly at low pressures in the stratosphere. Therefore, the atmosphere is optically thin in the 9.6-μm band and the absorption follows the weak line approximation (Plass, 1958). Thus, all the weighting functions obtainable for this gas, in the 9.6-μm absorption band, have essentially the same shape and closely resemble the shape of the vertical ozone profile itself (Prabhakara, 1969). Hence, detailed information cannot be obtained regarding the vertical distribution of ozone from the spectral measurements made in this band. It is necessary, therefore, to take advantage of some of the climatological statistical properties of the ozone profile in any remote sounding method.

Ozone profiles differ significantly in tropical and extratropical latitudes, primarily because of the abrupt change in the height of the tropopause at about 30°N and 30°S. So, the mean and the characteristic patterns (e.g., Holmstrom, 1963) of the ozone profile have been derived separately for tropical and extratropical latitudes from ozone sounder observations over North America (Hering and Borden, 1965, 1967). In Figure 1 the mean profile and the first characteristic pattern (CP_1) are shown for both the tropical and extratropical latitudinal zones. These two climatological properties are

*Heath, D., Mateer, C. L., and Krueger, A., 1971. Private correspondence.
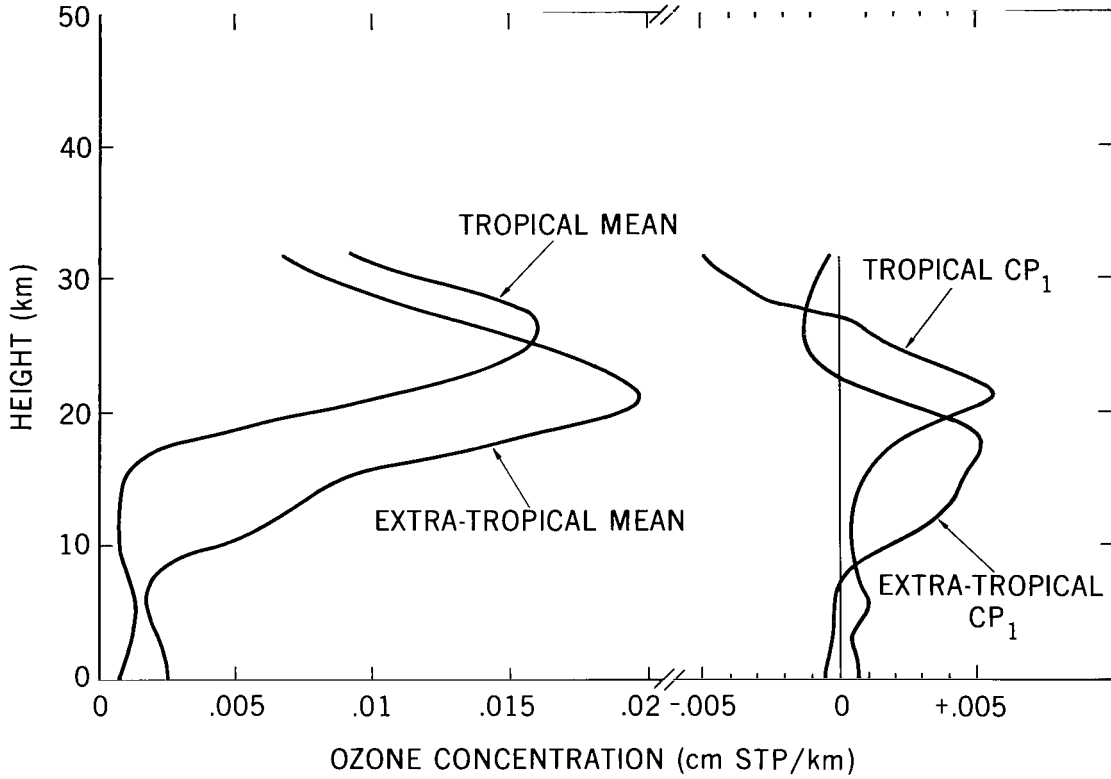
Figure 1—The mean and the characteristic pattern of ozone profile.

used to represent the vertical profile in our remote ozone sounding method. Specifically, the distribution of ozone with height z in a given latitudinal zone is assumed to be given by

$$O_3(z) = \overline{O_3}(z) + \alpha_1 \, f_1(z) \tag{1}$$

where $\overline{O_3}(z)$ and $f_1(z)$ are respectively the mean and the CP_1 value for the latitudinal zone. The parameter α_1 in Equation 1 characterizes the ozone profile. Thus, the objective of our remote ozone sounding method is to determine this parameter from the IRIS 9.6-μm spectral measurements by suitably applying the radiative transfer formalism.

The radiative transfer equation in a nonscattering atmosphere under local thermodynamic equilibrium may be written as

$$I_\nu = B_\nu [T(z_0)] \tau_\nu(z_0) + \int_{\tau_\nu(z_0)}^1 B_\nu [T(z)] d\tau_\nu(z) \tag{2}$$

where ν is the wave number; B_ν is the Planck intensity, $T(z_0)$ and $T(z)$ are the absolute temperatures at the surface and any height z in the atmosphere; and $\tau_\nu(z_0)$ and $\tau_\nu(z)$ are the transmissions from the surface and from any level z to the top of the atmosphere.

5

In Equation 2, the transmission function $\tau_\nu(z)$ can be expressed in terms of the ozone profile $O_3(z)$; for this reason, $\tau_\nu(z)$ becomes a function of the parameter α_1 via Equation 1. Now, since the temperature distribution $T(z)$ in the atmosphere can be obtained from the IRIS 15-μm spectral measurements (Conrath et al., 1970), Equation 2 can be readily solved for α_1. The total ozone is then obtained by a simple integration of the ozone profile with respect to height.

DISCUSSION OF TOTAL-OZONE CONTENT CHARTS AND RESULTS

Accuracy of Remote Ozone Soundings

The remote sounding method described in the previous section was applied to Nimbus 3 IRIS radiance measurements in the 15-μm and the 9.6-μm regions and ozone profiles were derived at several stations (see Prabhakara et al., 1970). Such derived profiles of ozone, in general, reproduce only crudely some salient features of the true profile. On the other hand, the vertically integrated total-ozone content is only quantitatively estimated. Figure 2 compares the total ozone derived from IRIS measurements with the Dobson measurements. The agreement between the two sets of measurements is quite encouraging. The standard error of estimate is about 6 percent with respect to the Dobson measurements.
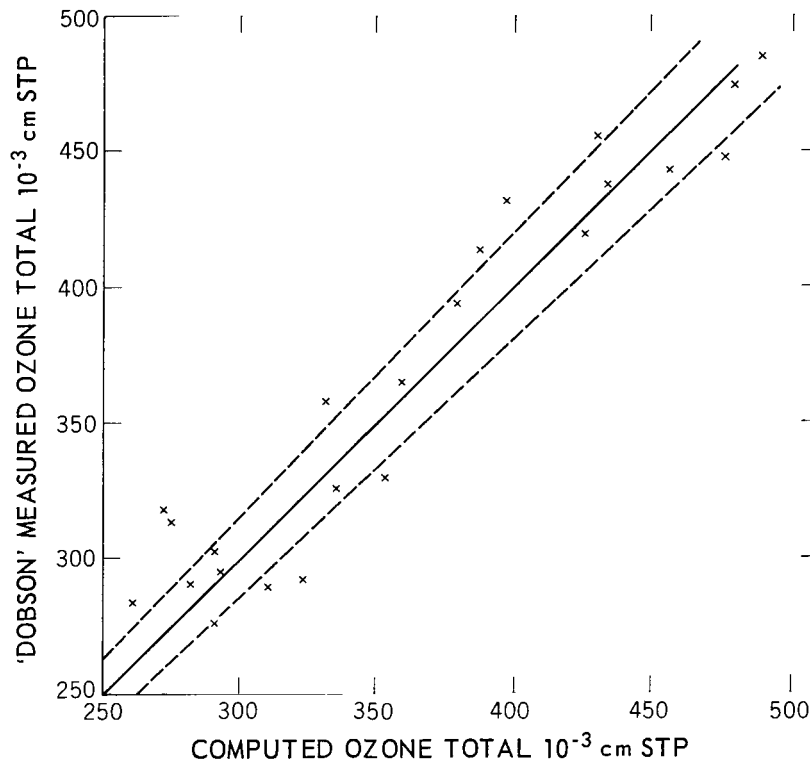
Figure 2—Computed total-ozone content (Nimbus 3 IRIS data) versus Dobson measured ozone concentration.

Remote sounding in the infrared (5-20 µm) cannot measure the lower-tropospheric water vapor and temperature distribution through clouds. This limitation arises largely because the infrared spectrum does not provide the information needed for delineation of the physical parameters of the clouds. * Remote sounding of ozone, on the other hand, does not suffer from this limitation because the ozone layer is mainly above the tropopause and, to a first approximation, may be considered to be physically separated from tropospheric water vapor, aerosols and clouds. This stratification greatly aids the simplification of radiative transfer considerations, as shown in Prabhakara et al. (1970), and hence the vertical distribution of ozone, characterized by one parameter, can be obtained even in cloudy sky conditions. However, when the clouds are present at very high altitudes in the troposphere, the cloud-top temperatures tend to be low. Such a cold radiative background, in general, reduces the spectral intensities to a small value, and the signal-to-noise ratio under such conditions can be unduly large. Errors in the estimation of ozone could be large with a noisy set of radiance values. A similar circumstance is also encountered when the ground is very cold (<240 K), such as over Antarctica.

In order to illustrate some of the effects mentioned above, Figure 3 shows the total-ozone variation along the track of orbit 114 (midnight, April 22, 1969) of the Nimbus 3 satellite. The orbital track shown in Figure 3(a) goes south, starting from about 80°N and 160°E and proceeding to 80°S and 15°W, crossing the equator around 75°E. The ozone curve in Figure 3(b) actually connects data points that are spaced about 1 deg of latitude apart. The lower curve in Figure 3(b) gives the corresponding brightness temperatures sensed by IRIS in the water-vapor window region around 10.5 µm. The brightness temperatures are plotted with a negative ordinate for easier presentation. The sharp decreases in the brightness temperatures vividly reveal the presence of clouds along the orbital path. Now, if the ozone curve is examined in conjunction with the brightness curve, a systematic association cannot be discerned between the clouds and the remotely sensed ozone. However, the probable presence of high clouds, as indicated by a low brightness temperature (<237 K) around 6°N, could

---

*A factor (statistical) analysis has been performed on the information content of the 15-µm spectral measurements of Nimbus 4 IRIS, which has a resolution of 2.8 cm^{-1} and an rms error in intensity measurements of about 0.5×10^{-7} joule-cm^{-1}-sec^{-1}-$ster^{-1}$. In two different samples of spectra, one for clear skies and the other for cloudy skies, only four significant pieces of information were found above the noise level. This finding shows that the clouds do not add extra information.

So that the implications of the above analysis could be comprehended further, another test was performed with the help of synthetically computed 15-µm radiances for a few atmospheric models of temperature and the water-vapor distribution. For each model atmosphere, radiances were computed synthetically with clear sky, and also with clouds whose heights and amounts were varied in a systematic fashion. The clouds were assumed to be black, in the infrared, radiating at the ambient temperature of the air near the cloud top. Only two parameters, namely height and amount of the clouds, were chosen—the poorly known emission, transmission, reflection, and absorption characteristics were disregarded to simplify these calculations. The simulated spectra showed that widely different combinations of cloud heights and amounts can be chosen, yet the synthetic radiances for such combinations will differ by no more than the noise level of 0.5×10^{-7} joule-cm^{-1}-$ster^{-1}$-sec^{-1}.

These tests conclusively show that it is not possible to derive a solution of the lower-tropospheric temperature distribution from 15-µm spectral measurements in cloudy skies without specifying some extra information, such as the ground temperature.
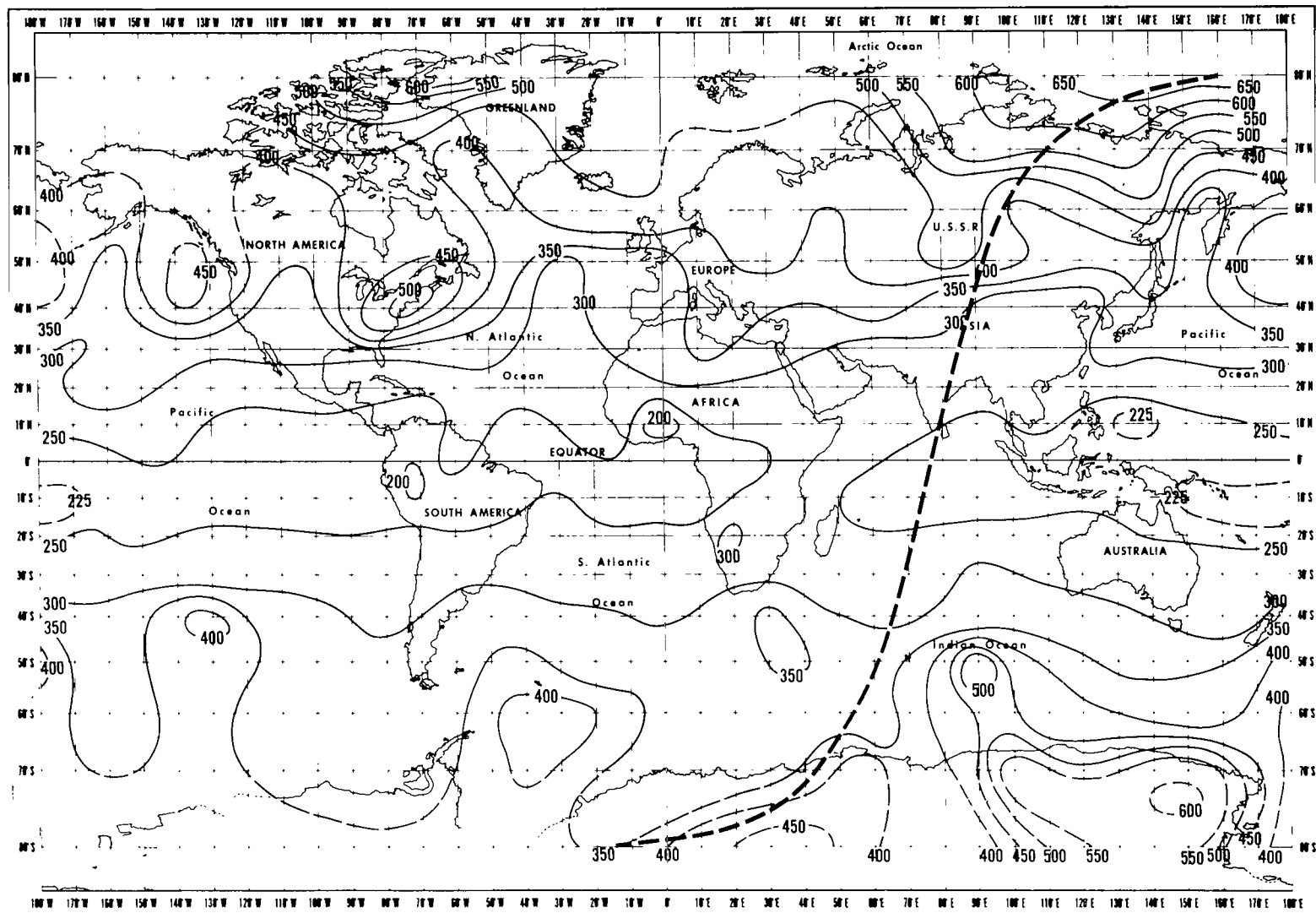
Figure 3(a)—Total-ozone content (10^{-3} cm STP), April 22, 1969, Nimbus 3 IRIS data, with orbit 114 (dashed line) superimposed.
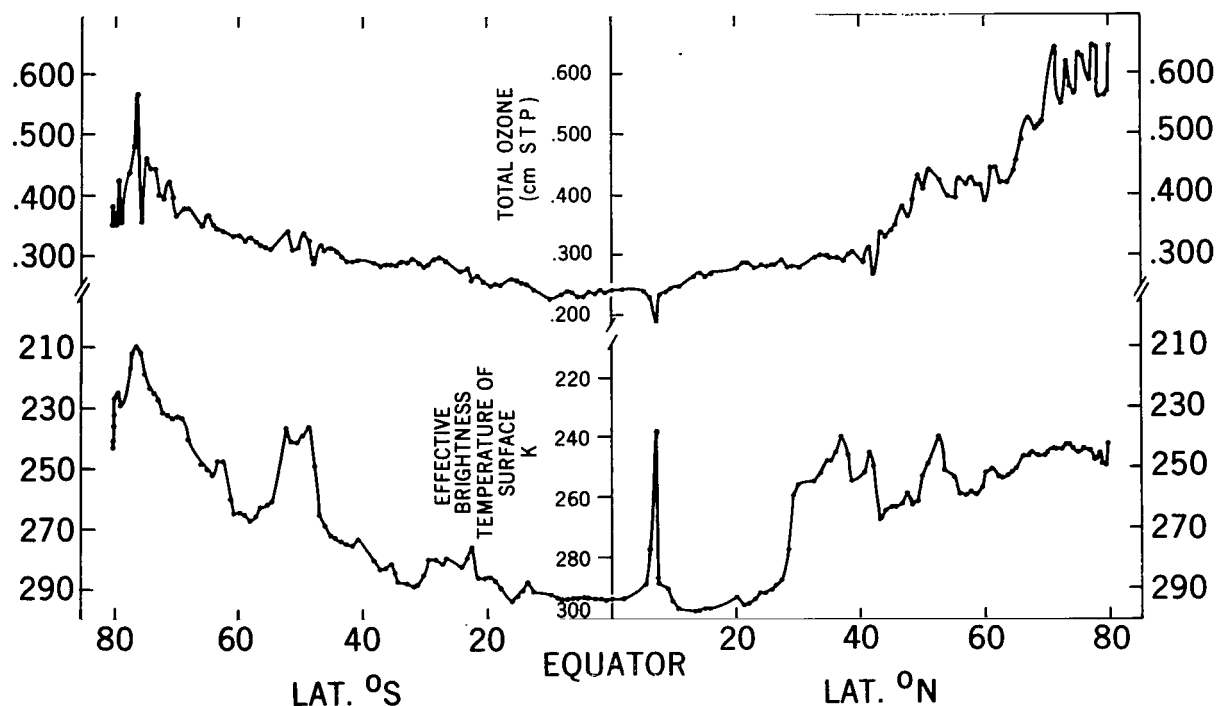
Figure 3(b)—Distribution of total ozone (cm STP) and effective brightness temperatures (K) of the surface and clouds along orbit 114, Nimbus 3 IRIS, April 22, 1969.

have introduced some error in the ozone value at that point. Unfortunately, a quantitative estimate of this error is not available. Also, in the Arctic region from 80°N to 70°N, where the brightness temperatures are around 245 K, a pronounced change in total ozone can be noticed, from about 650 units to 550 units, with an average of about 600. If these variations of ±50 around an average of 600 are assumed to be entirely due to random errors, then the random error in total-ozone measurements in the Arctic can be estimated at about 8.0 percent. Estimated values of total ozone over Antarctica, from 70°S to 80°S where the brightness temperatures are < 230 K, are particularly susceptible to larger errors.

Seasonal and Geographic Variations of Ozone

With the aid of this insight into the nature of the remotely sensed total-ozone data, the global, daily, total-ozone content maps derived from the IRIS data may now be examined.

As the numerical scheme used to invert the IRIS radiance measurements and obtain the ozone distribution is time-consuming on the computer (about 12 s for one inversion on an IBM 360/91), only approximately every fifth spectrum has been inverted. This method computed the ozone data separated by latitude intervals of approximately 5 deg.

9

The adjacent Nimbus 3 orbits are separated from one another by 107 minutes of time and about 26 deg of longitude at the equator. So, the coverage of the ozone data has a scale of 5 deg of latitude by 26 deg of longitude. With these data, global-ozone maps for eight days in April (22-29) and eight days in July (3-10) of 1969 have been analyzed. These maps are shown in Figures 4 and 5. Obviously, such maps are not synoptic in time. The orbital geometry might be expected to give radiance measurements around the globe as the time advances. But, whenever the orbits, which progress northward at local noon and southward at local midnight, cross the same geographic area 12 hours apart, the time sequence in the data is lost.

The ozone maps, in general, show an increase of ozone from the equatorial regions toward both the poles. In the equatorial regions, the values are around 0.25 cm, while in the Arctic regions during April (spring), values as high as 0.5 cm are frequently seen. On the other hand, during July (summer) the total ozone in the northern high latitudes is not as large. As explained earlier, the ozone data over Antarctica are not reliable.

In these daily ozone maps, several minima, maxima and troughs and ridges resembling the meteorological upper-air contour maps may be quickly noticed. However, the height values for upper-air contours generally decrease as the poles are approached, while the isolines of total ozone generally increase. This reflects clearly the inverse correlation between the two fields on a global scale. Such an inverse correlation was established by several earlier investigators with limited data.

So that the relationship between global total-ozone content changes and the meteorological parameters can be clearly seen, the 300-mb contour maps are compared with the ozone maps in Figures 4 and 5. This was the highest tropospheric level with sufficient upper-air data from both the northern (Free University of Berlin, 1969) and the southern (U.S. Navy, 1969) hemispheres. In the tropical regions, where no height data are available, the stream-function analysis has been displayed (NOAA, 1969). In this fashion, the 300-mb maps for April 22-29, 1969 (Figures 4(a) to (h)), and also for July 3-10, 1969 (Figures 5(a) to (h)), were constructed. These maps are all synoptic at 0000 GMT.

The ozone maps essentially reflect most of the features of the upper-air maps. The inverse correlation emphasized earlier is clearly shown; the pressure highs and lows at 300 mb correspond to ozone minima and maxima respectively. The same out-of-phase relationship is borne out in the ridges and troughs.

A lengthy descriptive account of the ozone and height maps day by day will be avoided here. So that any similarities may be comprehended, the ozone and 300-mb circulation maps for each day are presented on adjacent pages. In the left-hand parts of Figures 4 and 5 the 300-mb troughs are identified in both hemispheres and labeled with large letters. The ozone maxima corresponding to several of the 300-mb troughs are then shown with corresponding letters on the right-hand parts. The 300-mb

height maps are synoptic in time and scale, while the ozone maps are not. In spite of this very important difference between the two maps, several of the troughs may be identified and a reasonable progression of these troughs from day to day may be shown with the ozone maps. The middle and high latitudes of both the north and south hemispheres exhibit eight troughs in the ozone distribution, which corresponds to a general circulation regime of wave number 8. Although, as explained earlier, the total-ozone data over Antarctica are not quantitatively accurate, there is qualitative agreement between the 300-mb height maps and the ozone maps in the region from 60°S to 80°S.

In Figure 6, a mean map of the total ozone for eight days in April (22-29), 1969, is shown to bring out the climatology of the spring and fall in the northern and southern hemispheres, respectively. The mean map of ozone for eight days in July (3-10), 1969, shown in Figure 7, similarly emphasizes the climatology of the summer and winter seasons in the northern and southern hemispheres, respectively. A comparison of these two maps with the daily maps of ozone will readily show that there are many transient waves that do not appear in the mean maps. The semipermanent systems on the continents and oceans manifest themselves better in the mean map. The total ozone and its latitudinal gradient over the northern hemisphere decrease from spring to summer. The southern hemisphere, on the other hand, seems to show much less variation. The latitudinally-averaged total-ozone distribution shown for both the eight-day means in Figure 8 bears out this point quite vividly. This difference in behavior between the two hemispheres most probably stems from the greater oceanic coverage in the southern hemisphere.

CONCLUSIONS

The Nimbus 3 IRIS experiment has enabled the meteorologist to remotely sense, quite accurately, the total-ozone distribution over the globe except for Antarctica, where ozone measurements are only qualitative. The geographic coverage achieved by these data exceeds by far that offered by the sparse Dobson measurements. These daily and eight-day mean-ozone maps show several similarities and lend ample support to the seasonal maps of ozone constructed from Dobson data by London et al. (1962).

It has been shown that the ozone in the atmosphere is indeed a good tracer for upper-air motions on a global basis. The close relationship between the total ozone and the geopotential height of the 300-mb level, for example, could be used for several dynamic meteorological studies. For instance, the winds and heights at such levels could be indirectly deduced* from ozone data and fed into a numerical prediction model. In particular, for the vast tropical region and the southern hemisphere, where the conventional meteorological network for gathering upper-air data is sparse, the IRIS ozone measurements could be immensely valuable.

*Prabhakara, C., Rodgers, E., and Steranka, J. "Observations of Jet Streams over the Northern and Southern Hemispheres, from Nimbus 3 IRIS Ozone Data," in preparation at Goddard Space Flight Center, National Aeronautics and Space Administration, Greenbelt, Md.
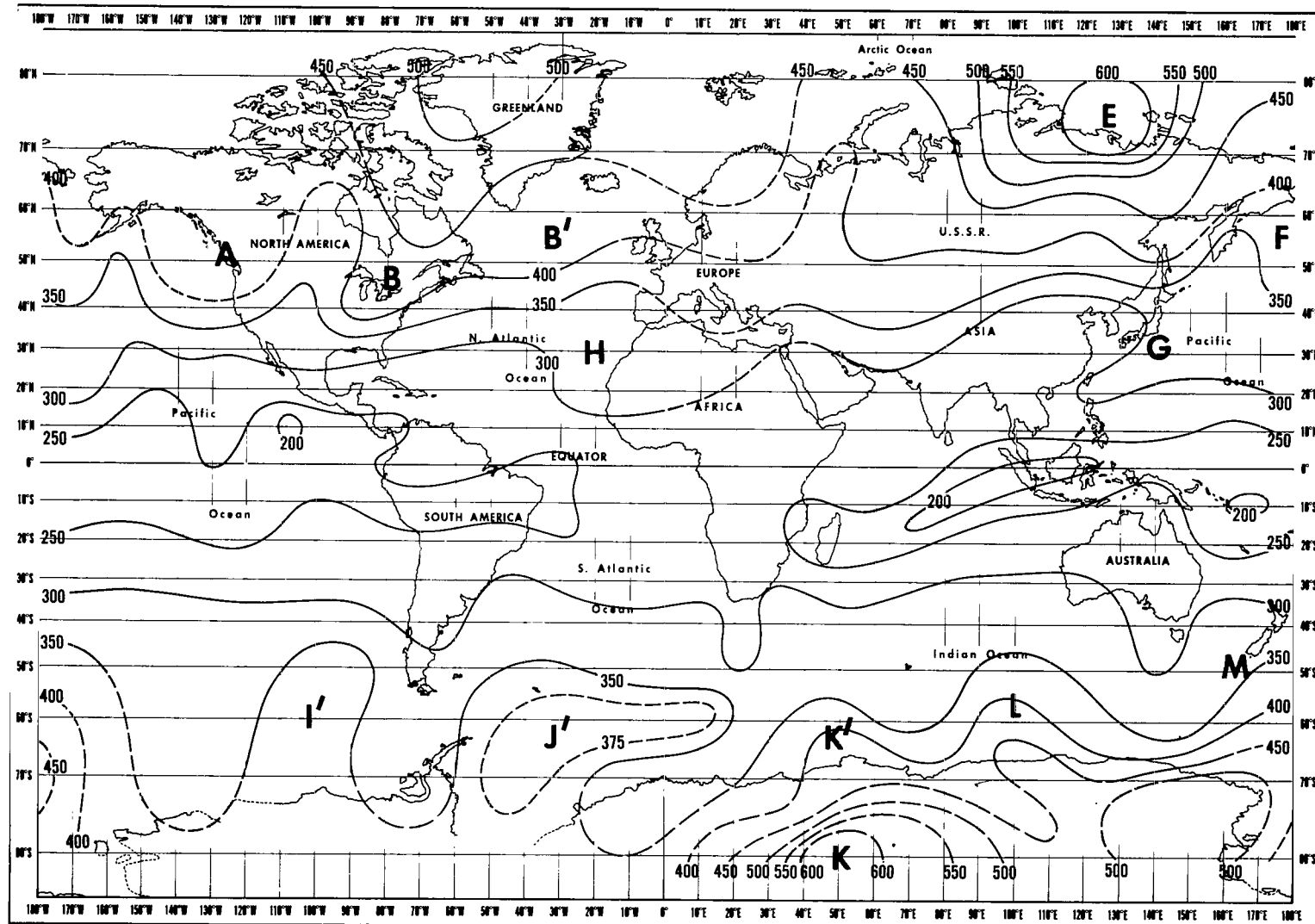
300-mb CHART, 0000 GMT
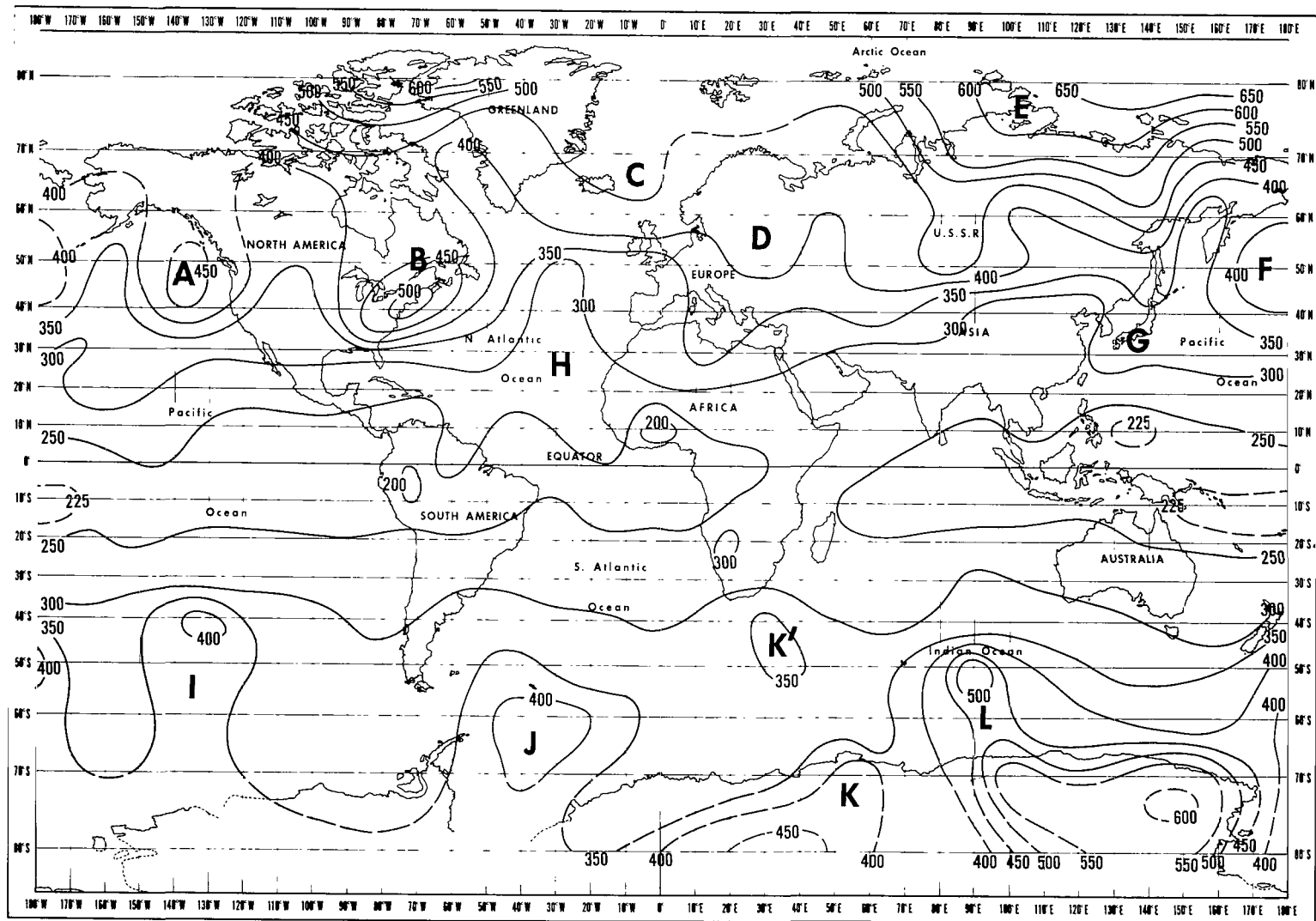
TOTAL-OZONE CONTENT (10⁻³ cm STP), NIMBUS 3 IRIS DATA

Figure 4(a)—April 22, 1969.

300-mb CHART, 0000 GMT
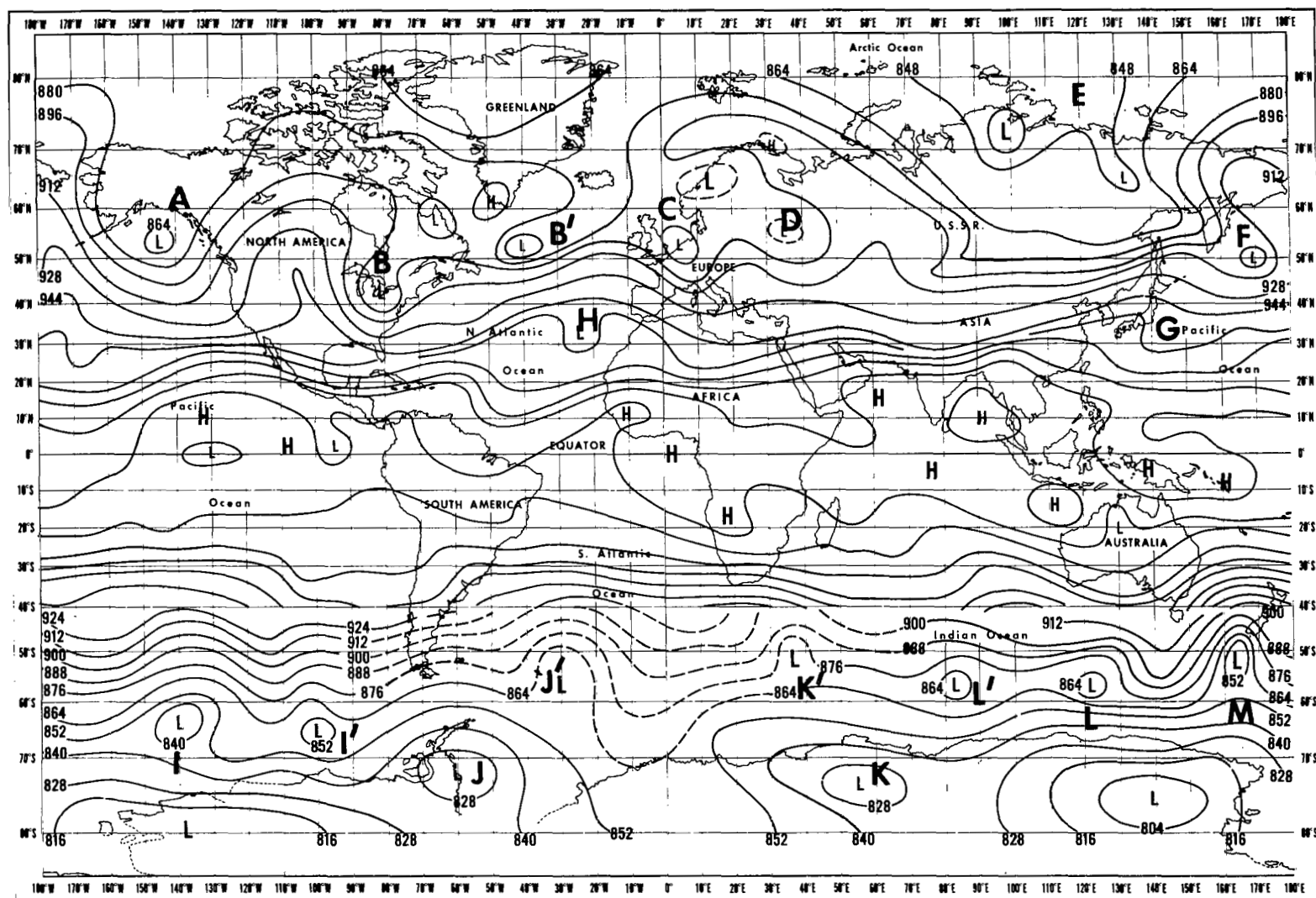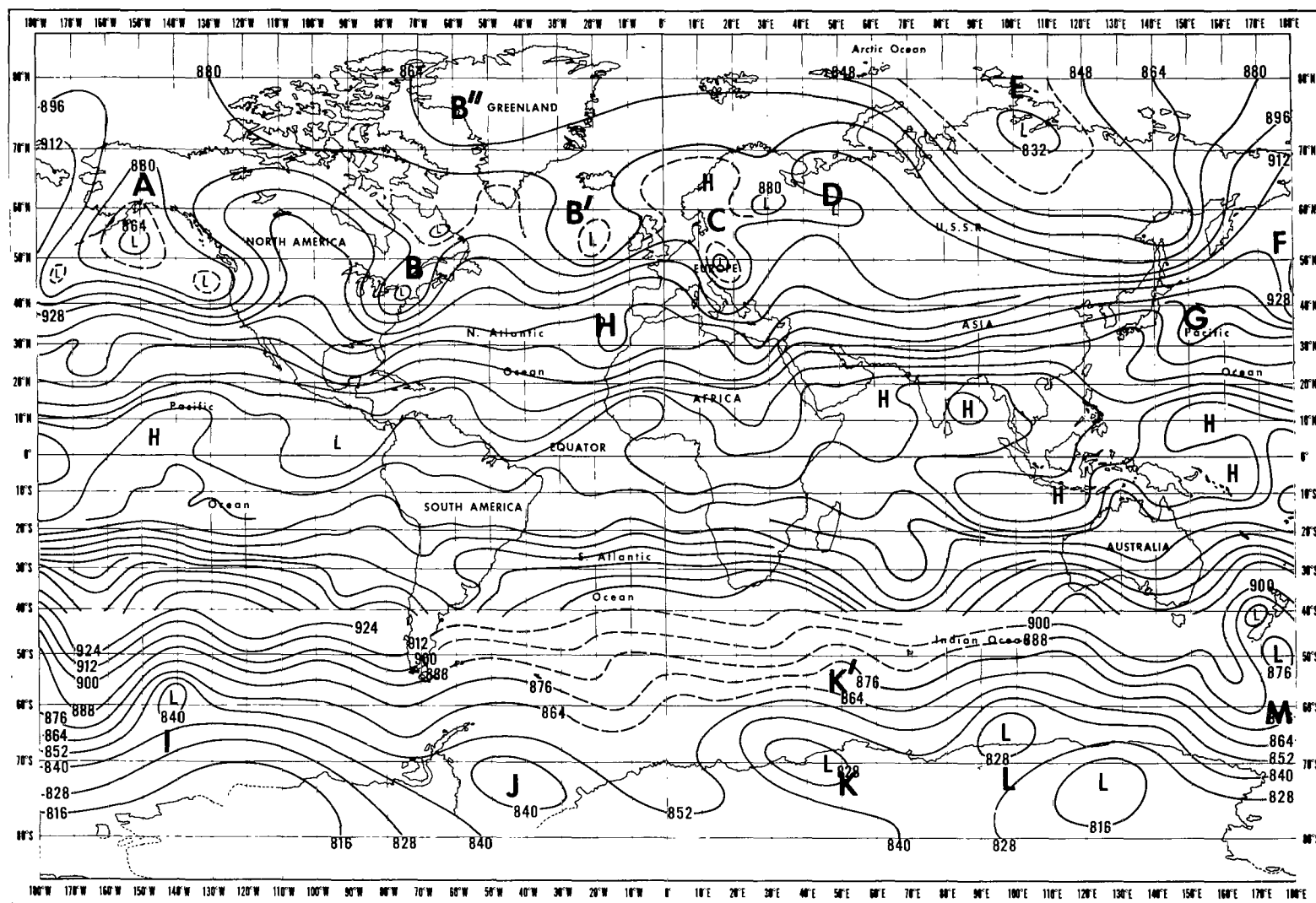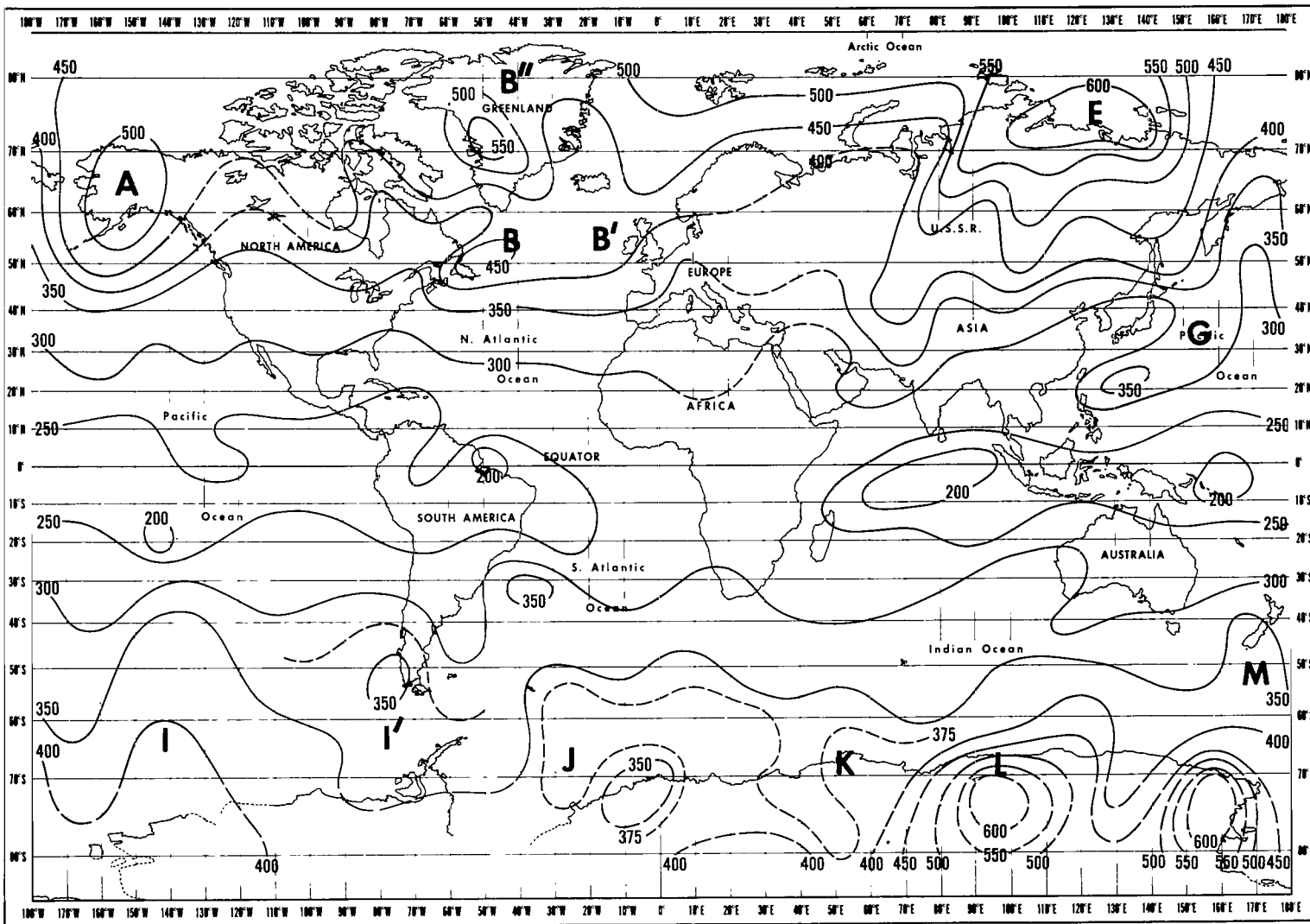
TOTAL-OZONE CONTENT (10^{-3} cm STP), NIMBUS 3 IRIS DATA
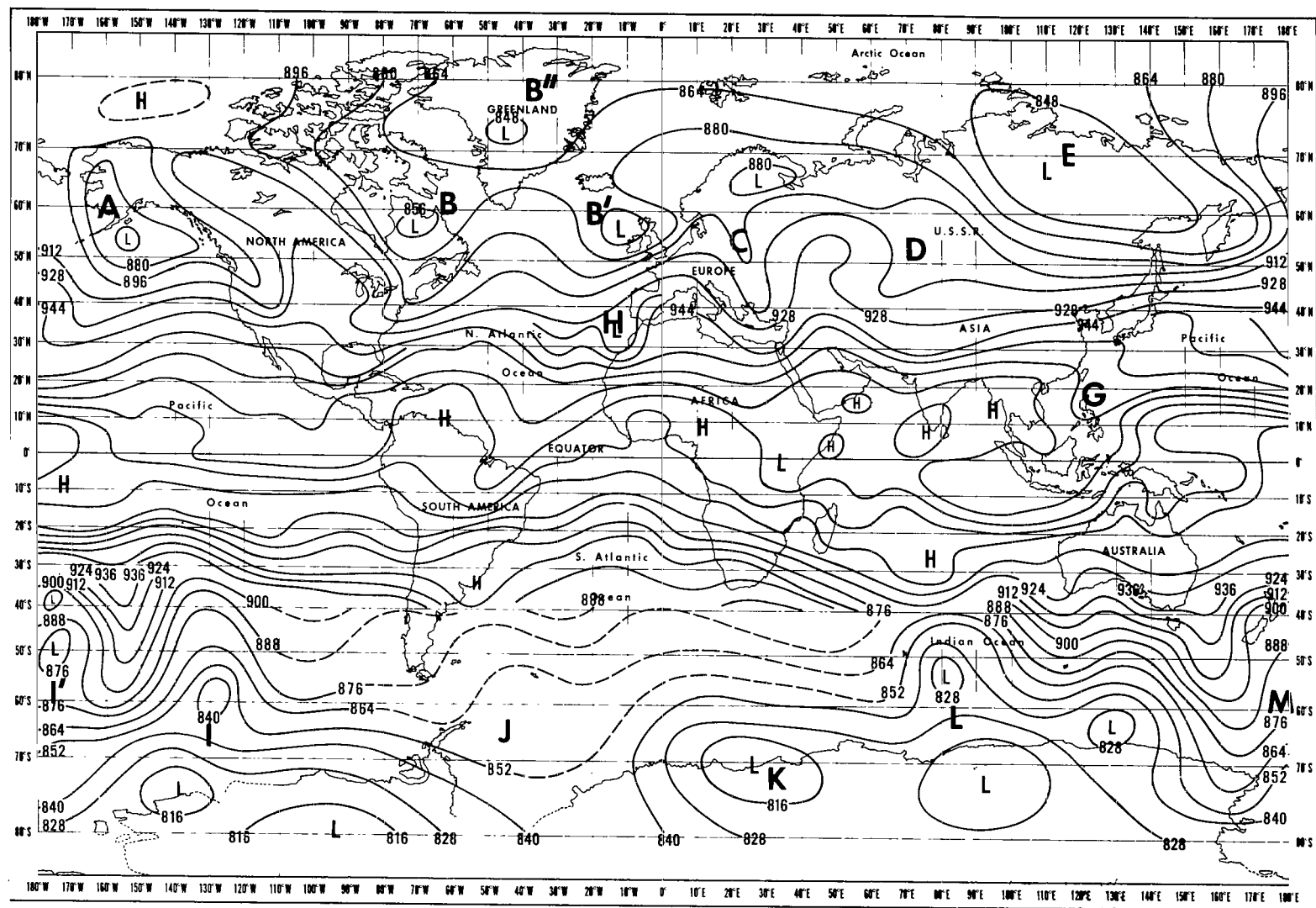
Figure 4(b)—April 23, 1969.
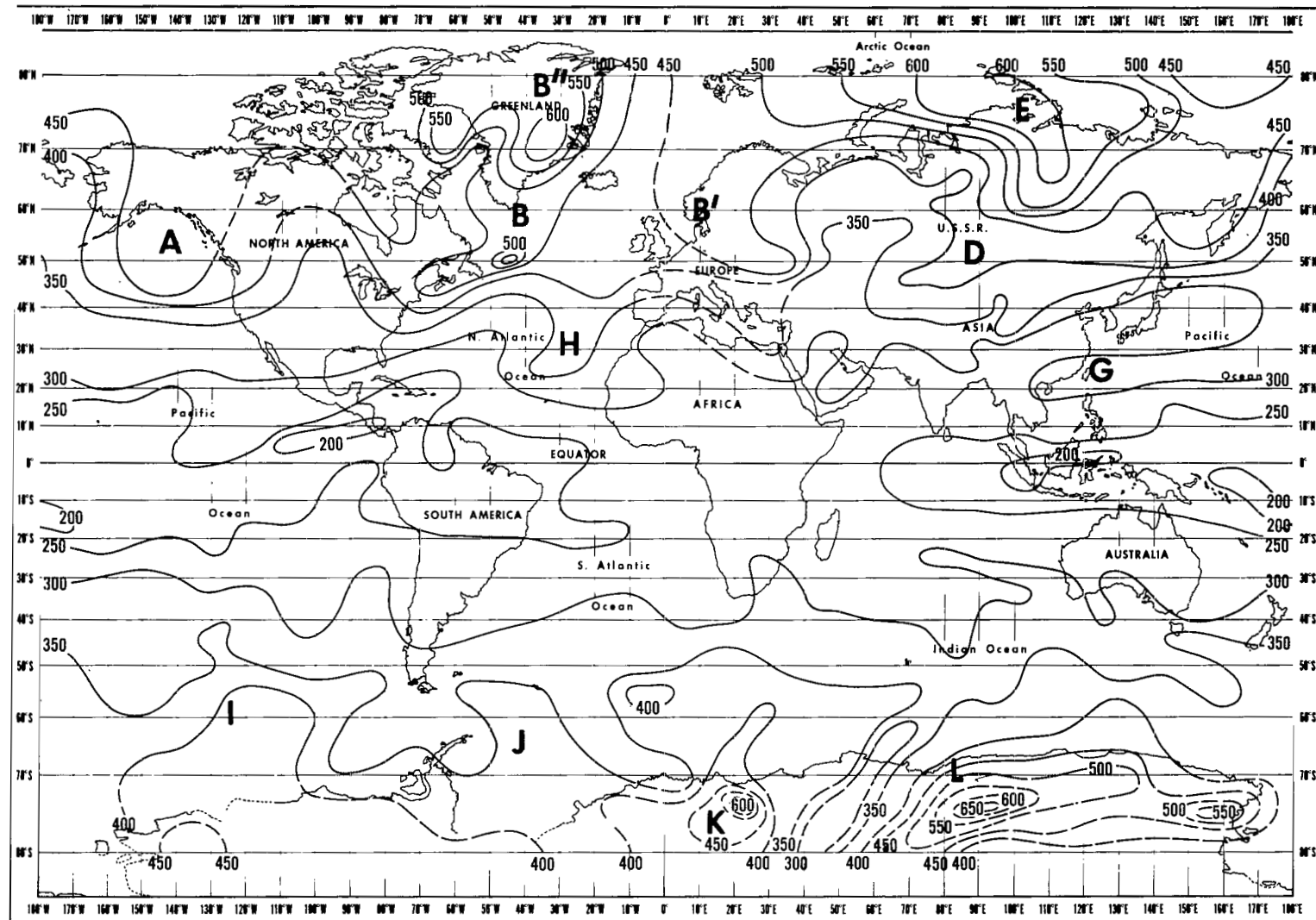
300-mb CHART, 0000 GMT

TOTAL-OZONE CONTENT (10^{-3} cm STP), NIMBUS 3 IRIS DATA
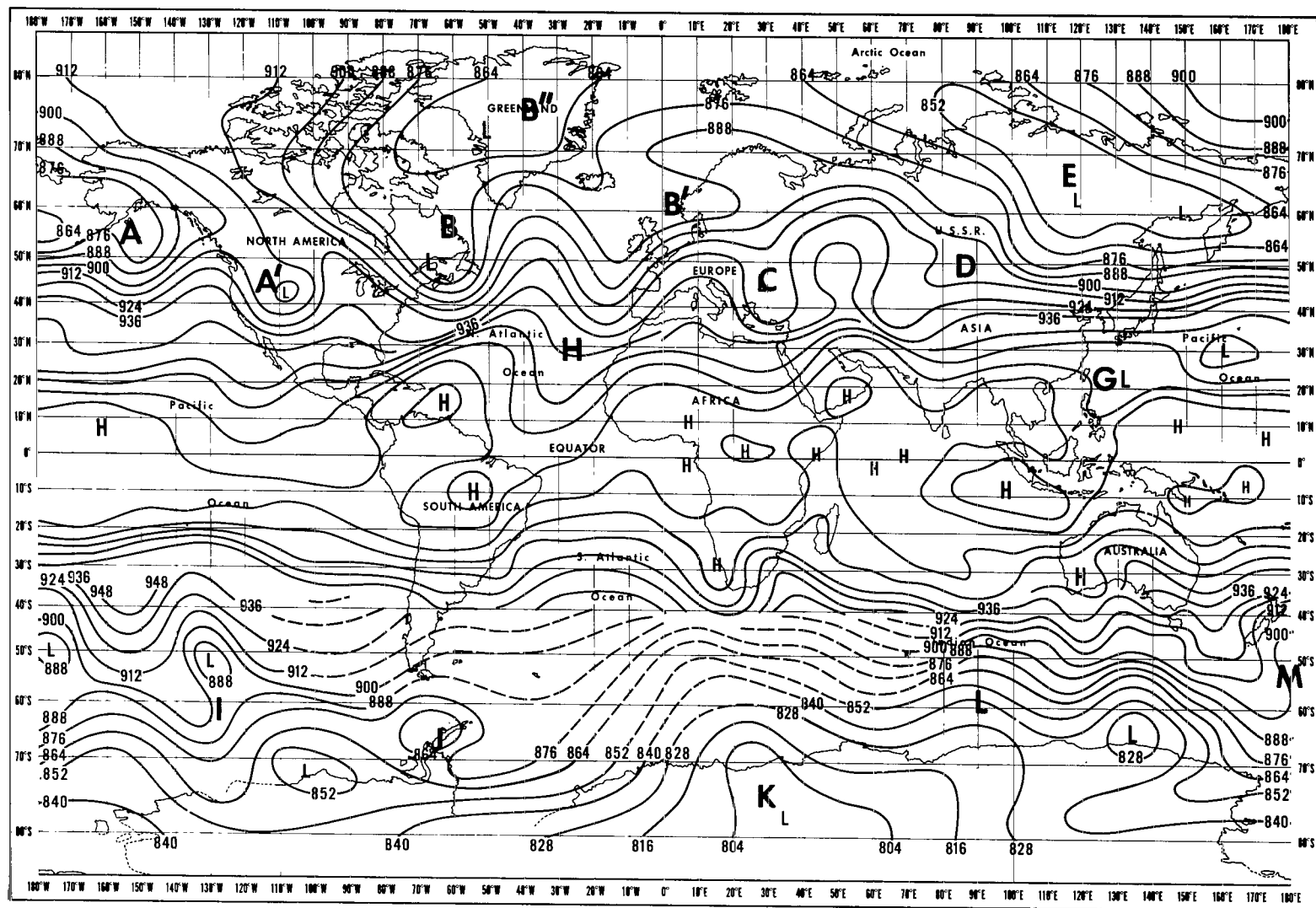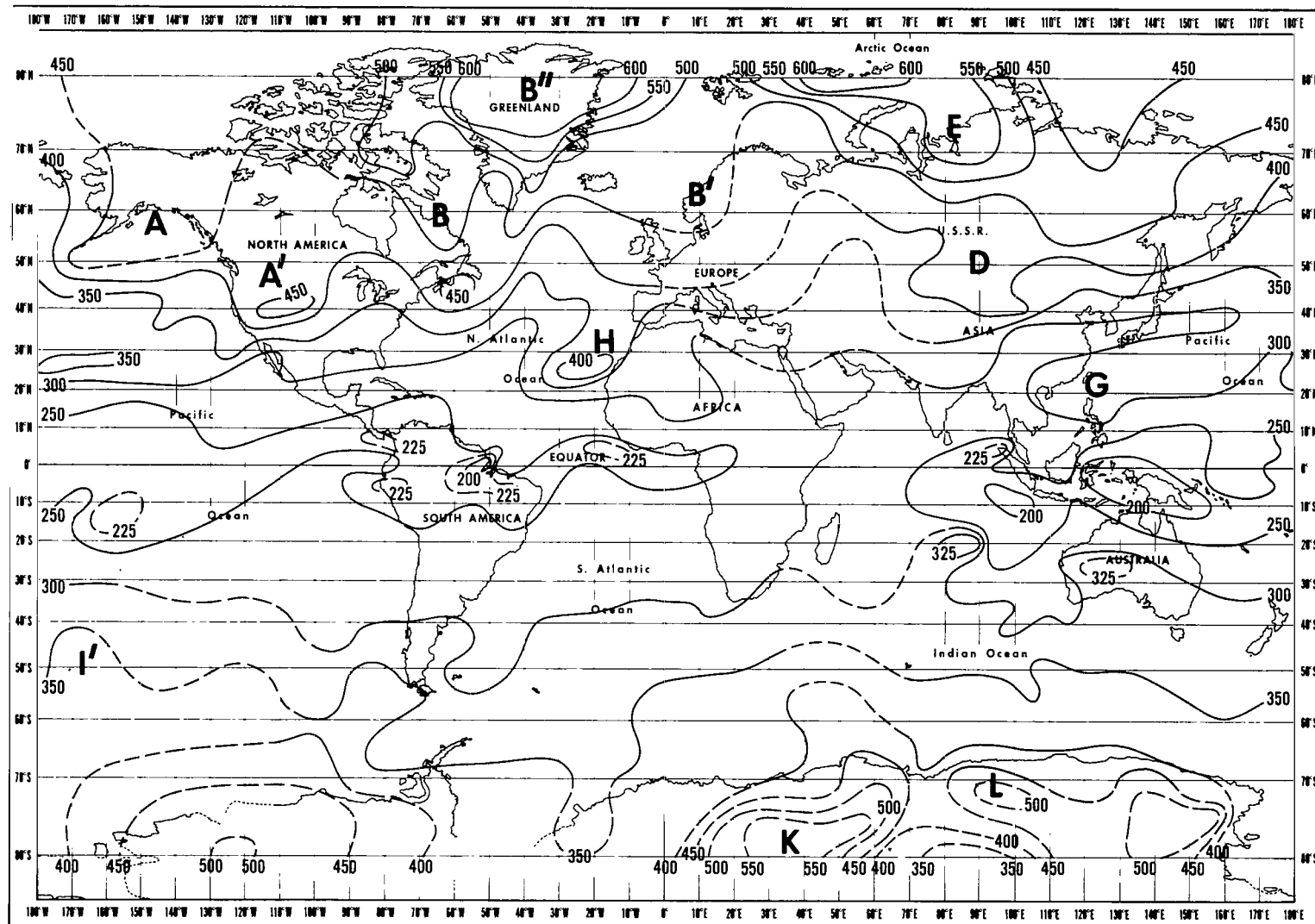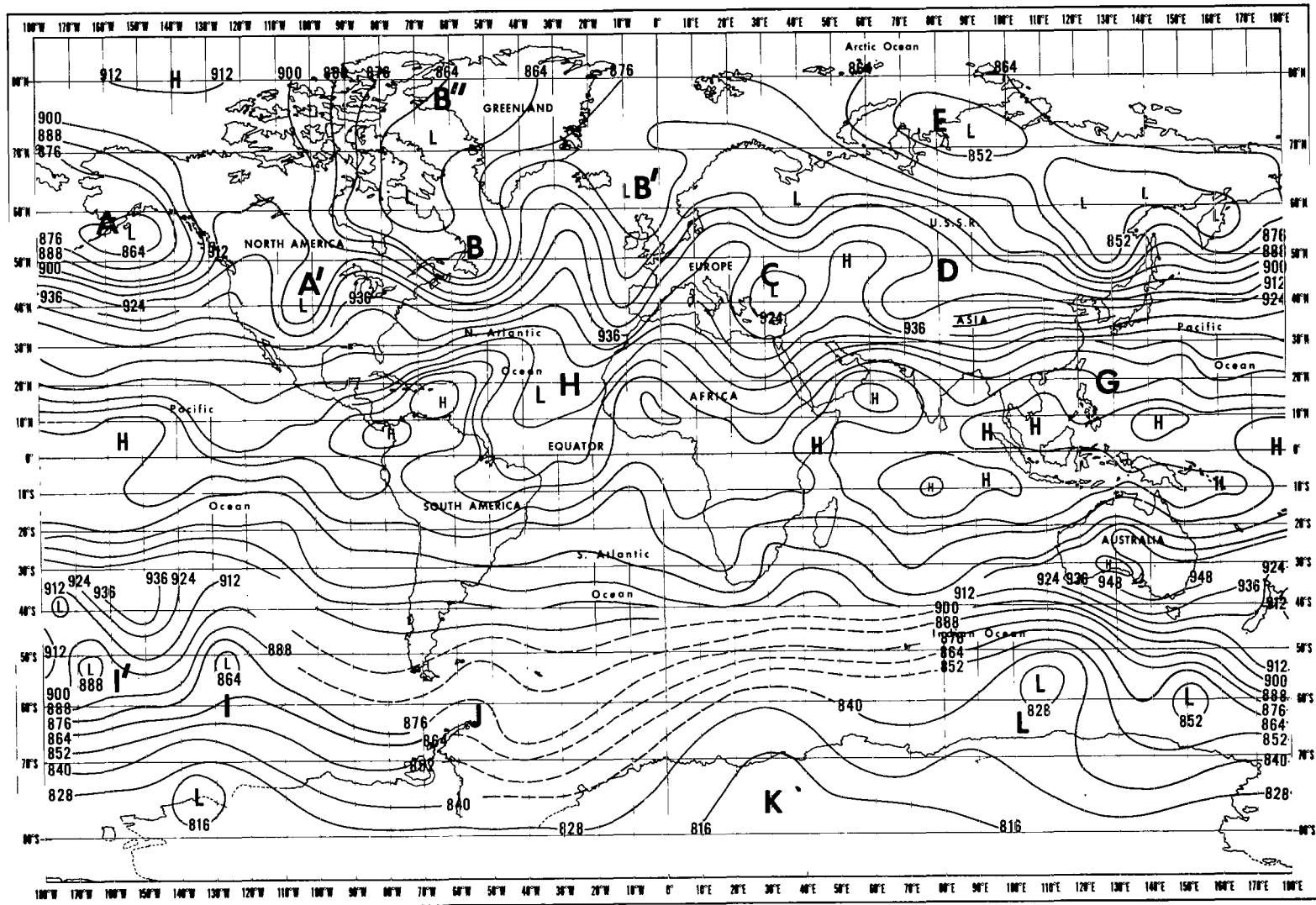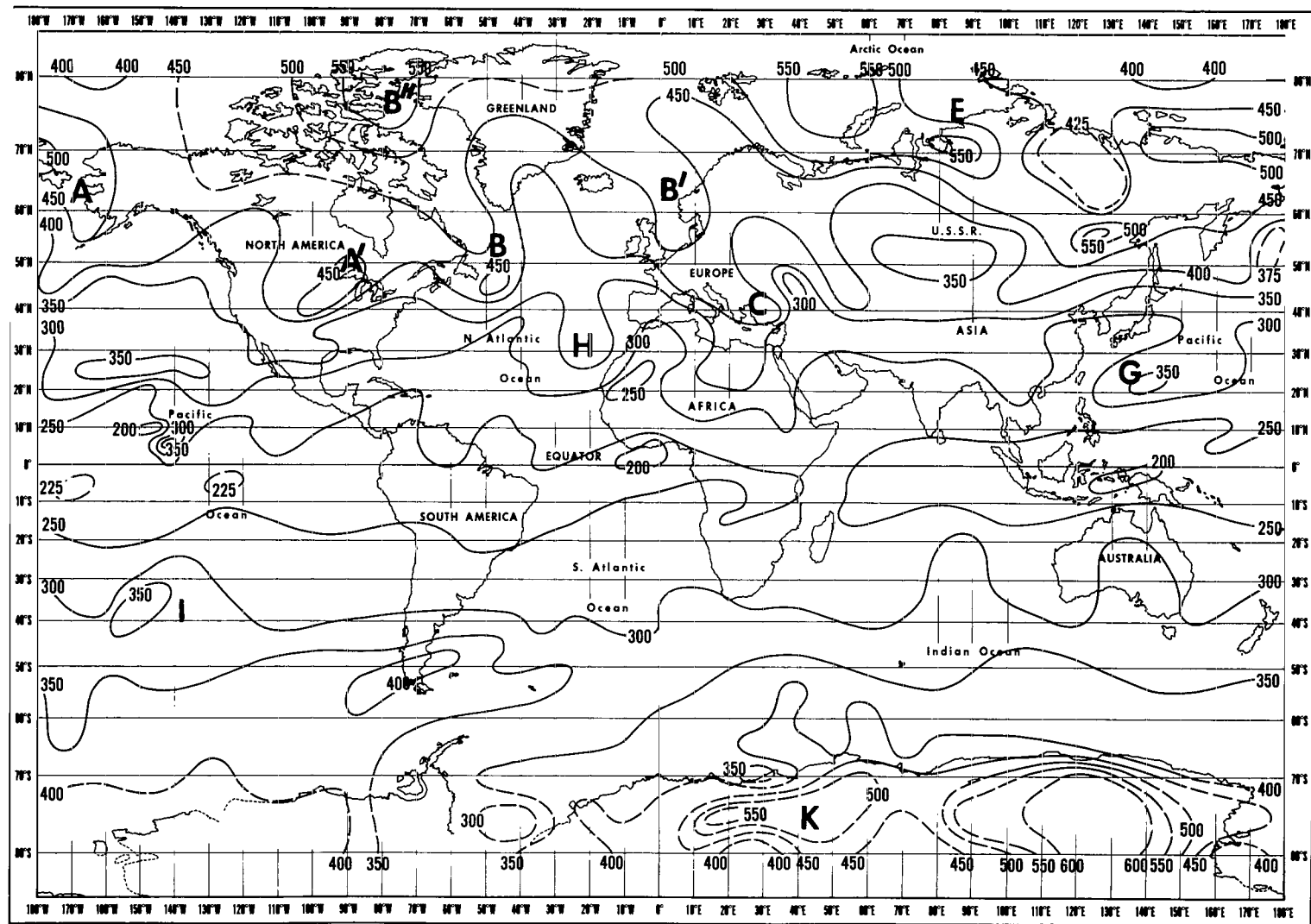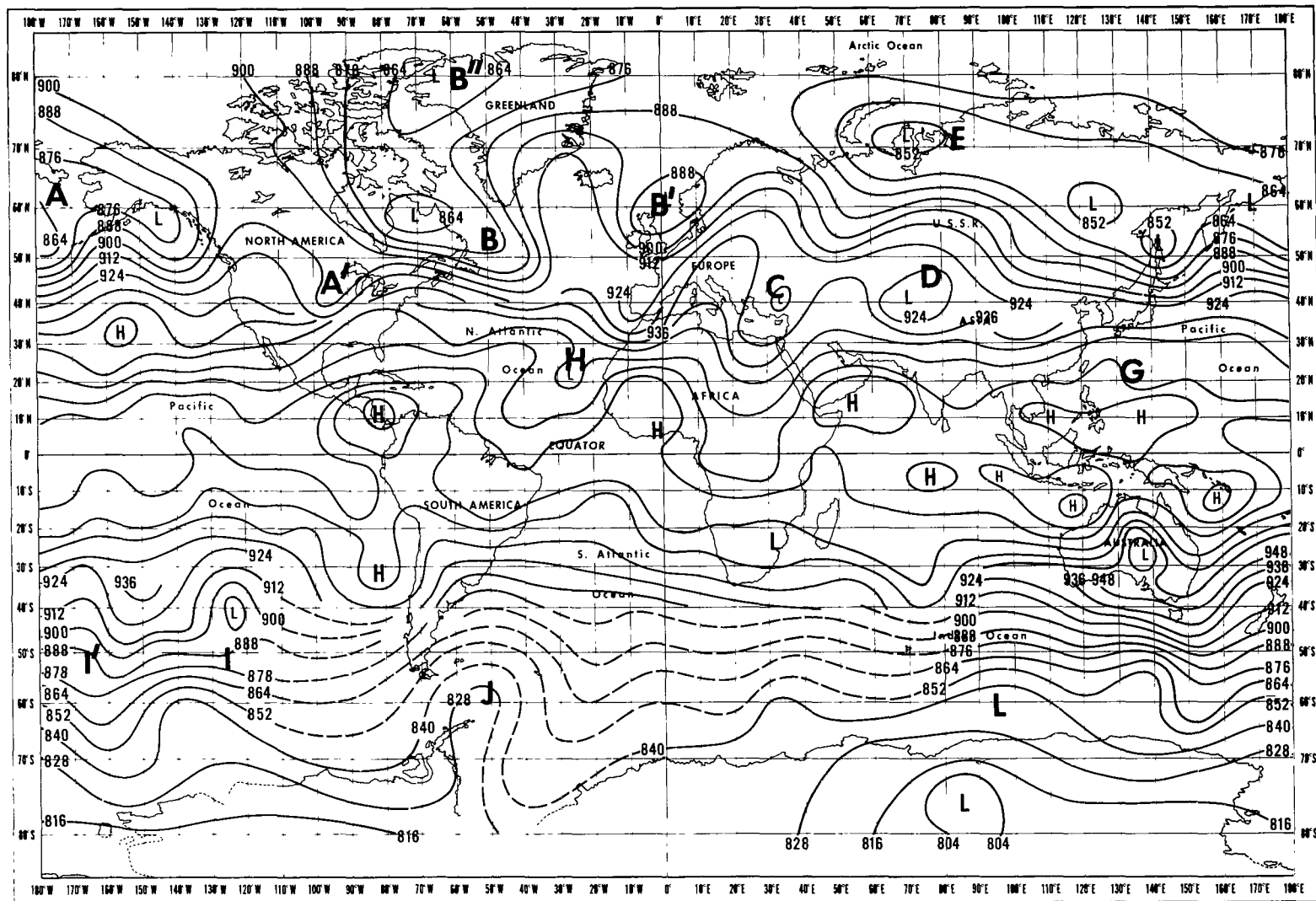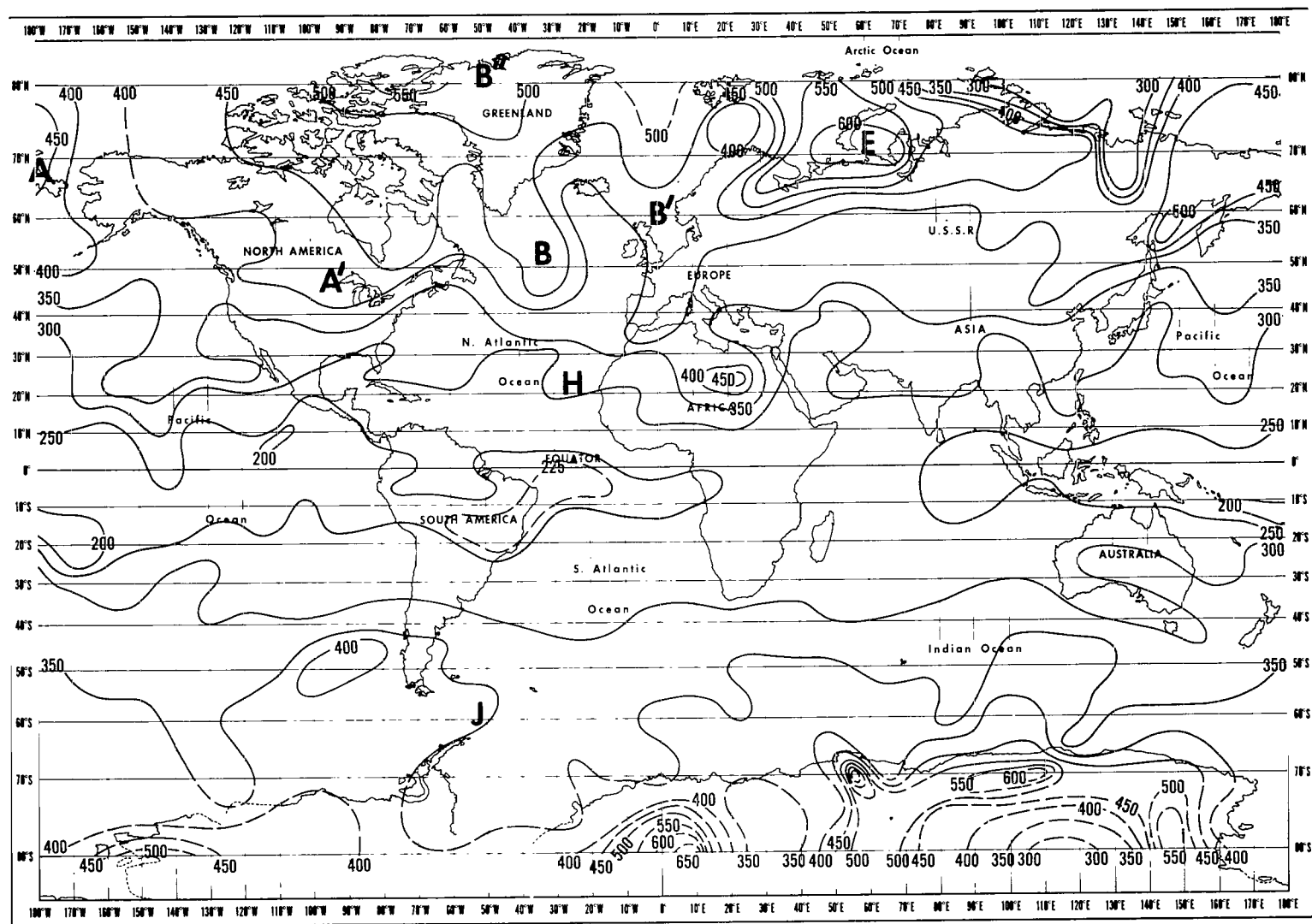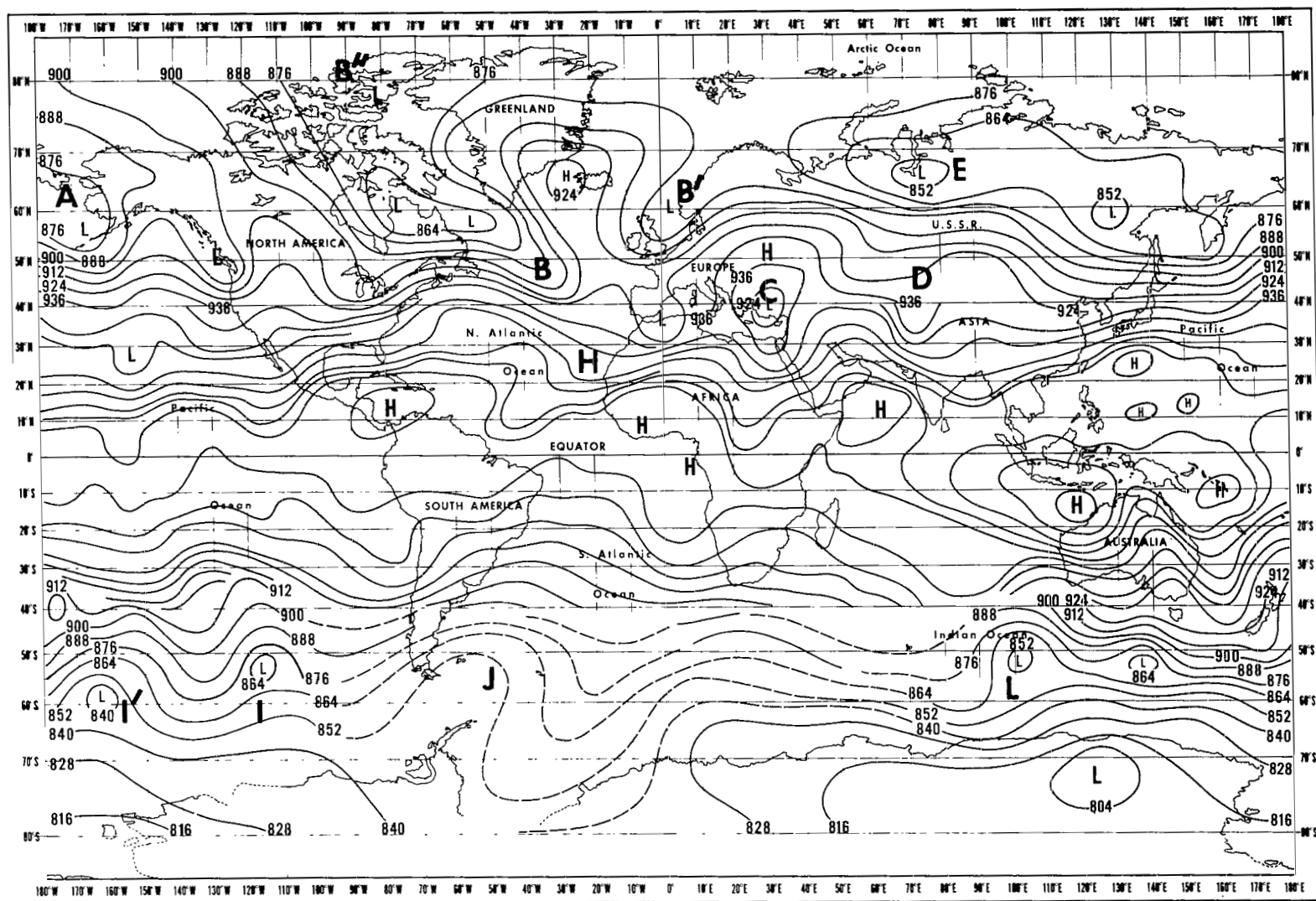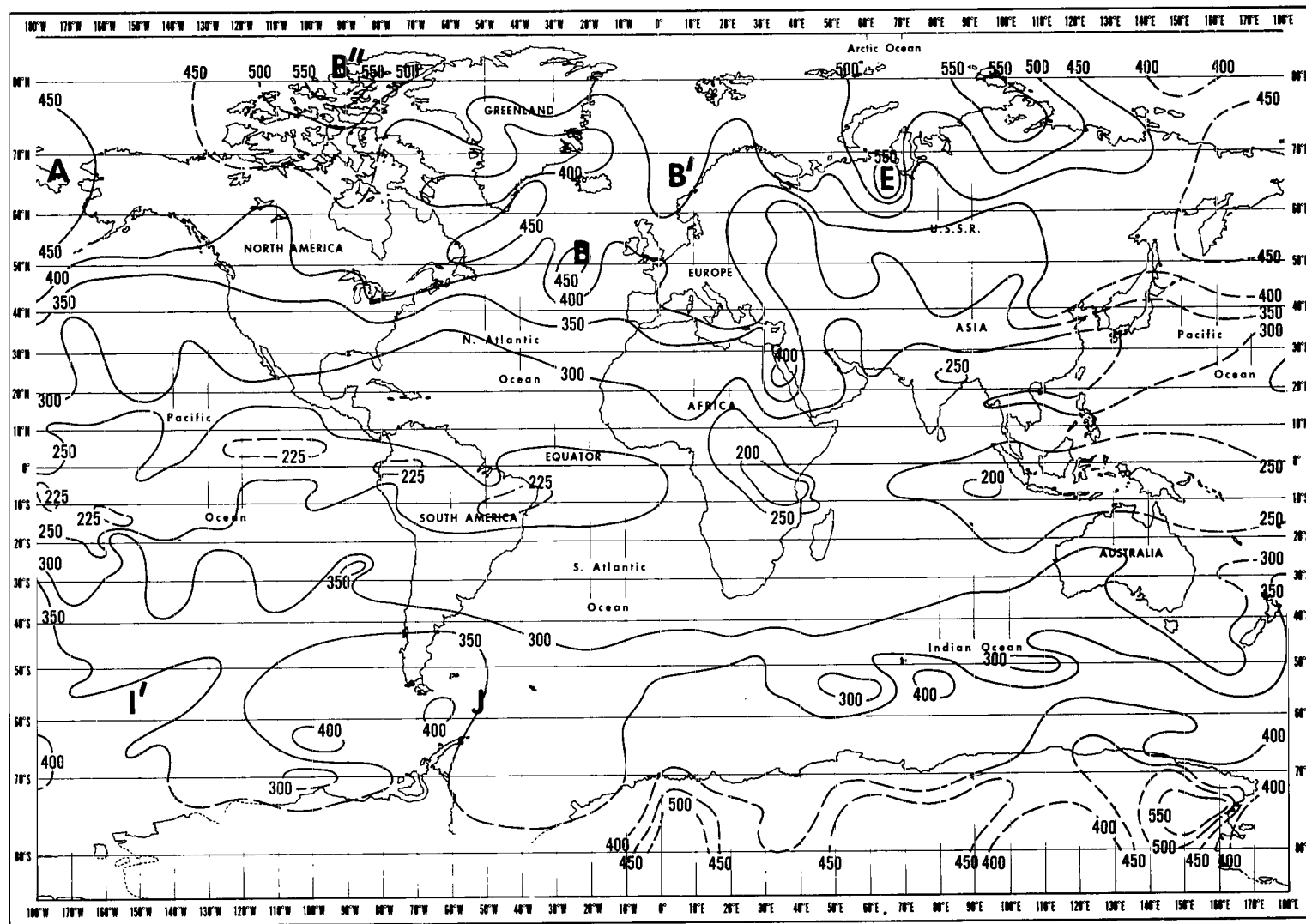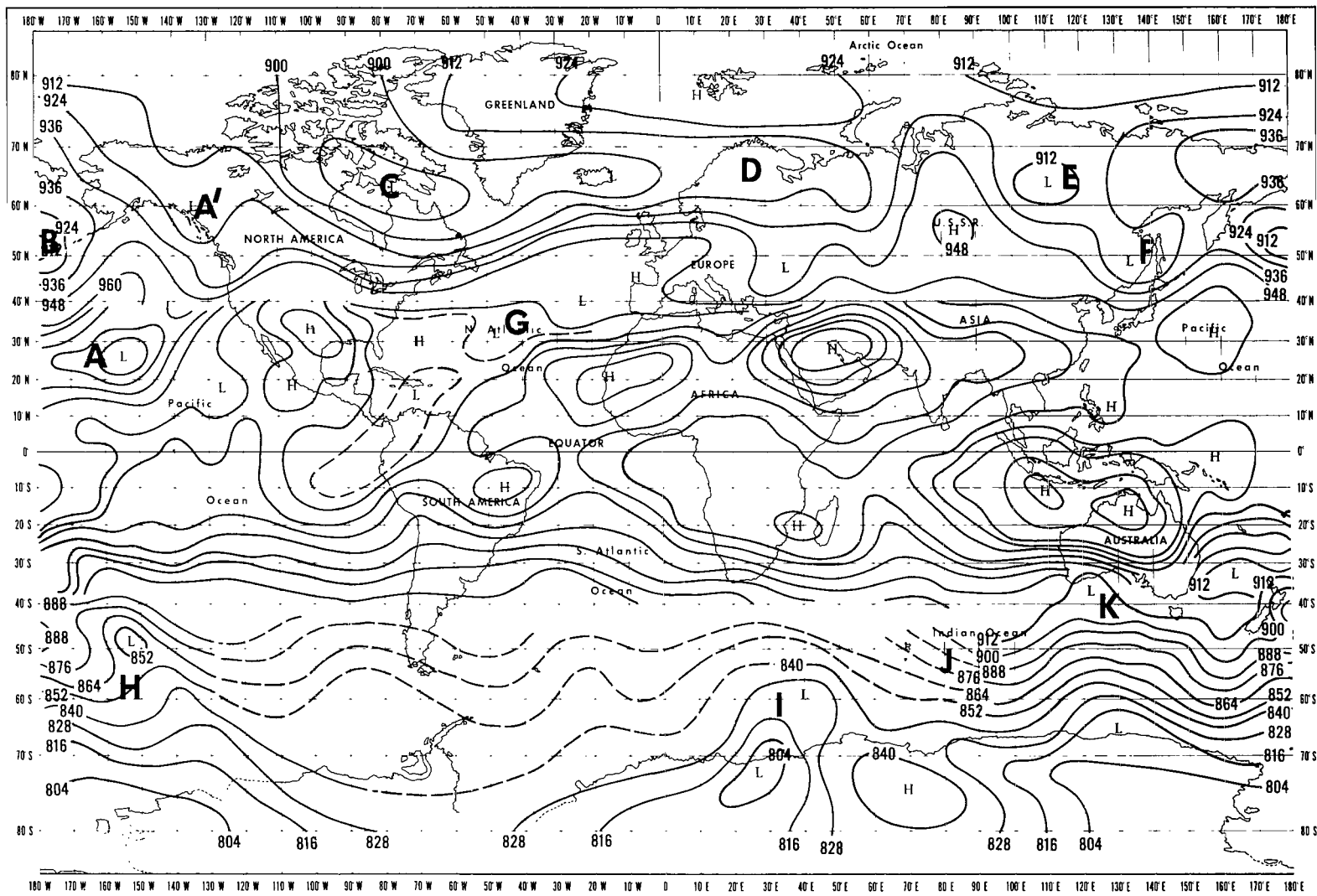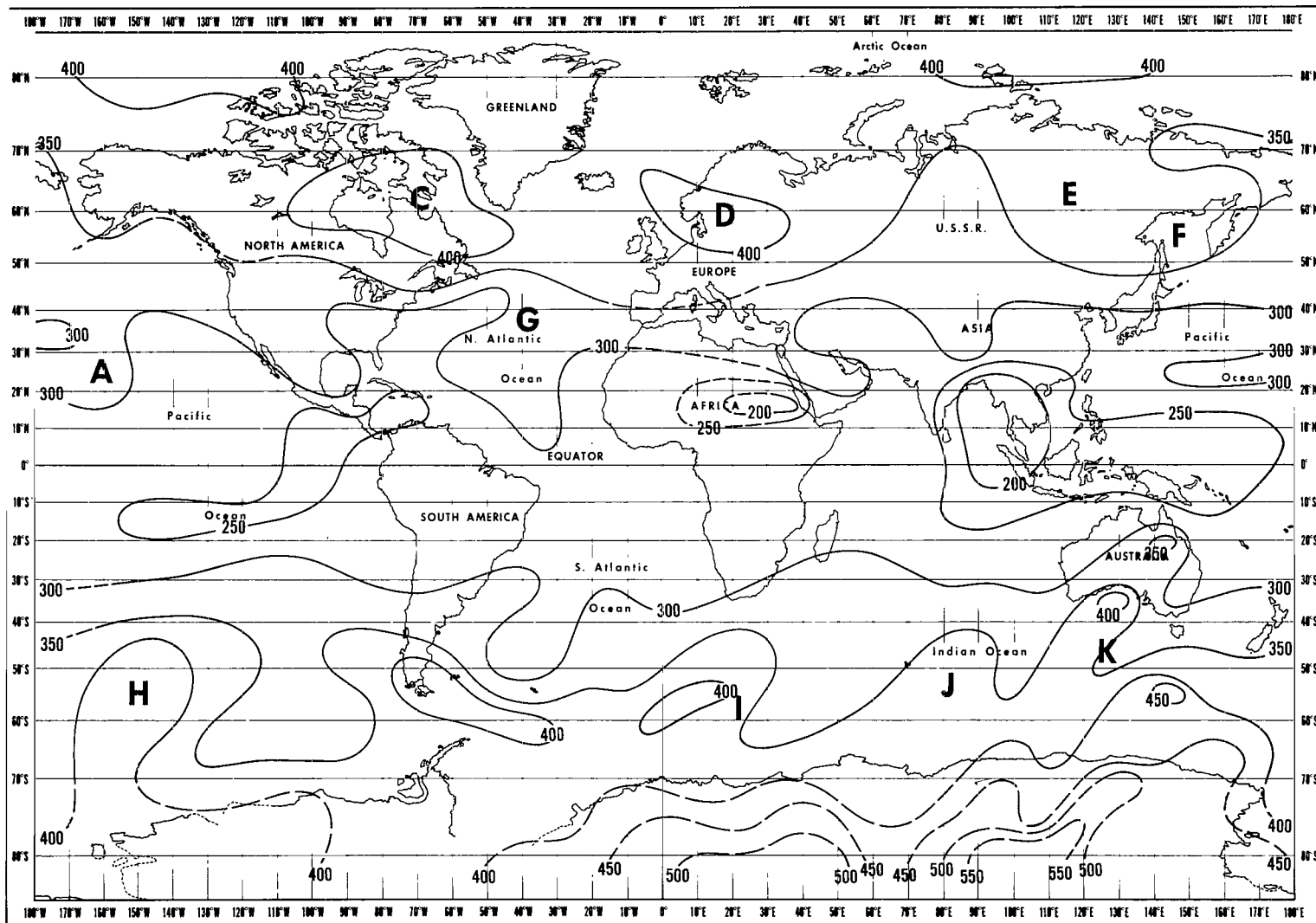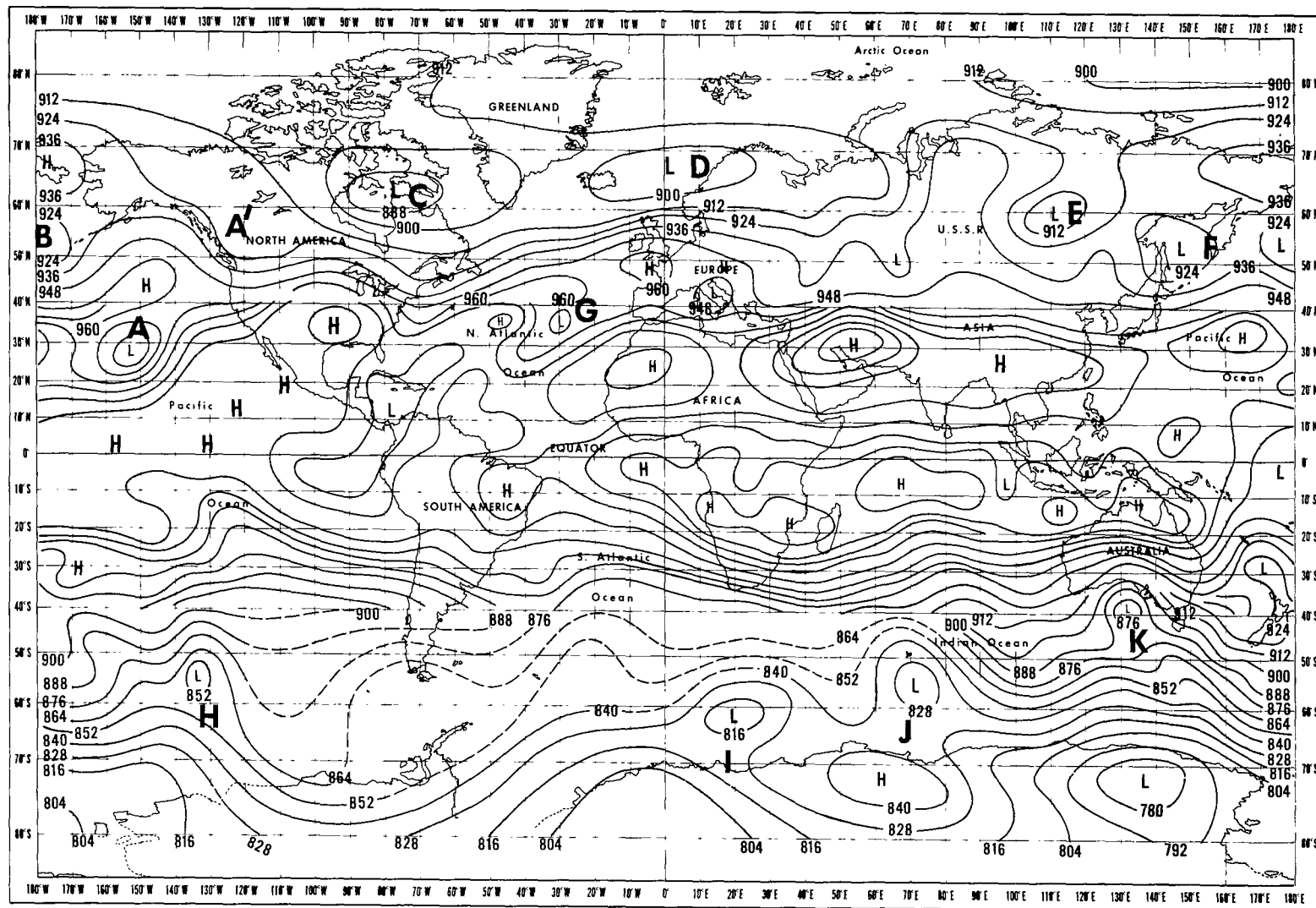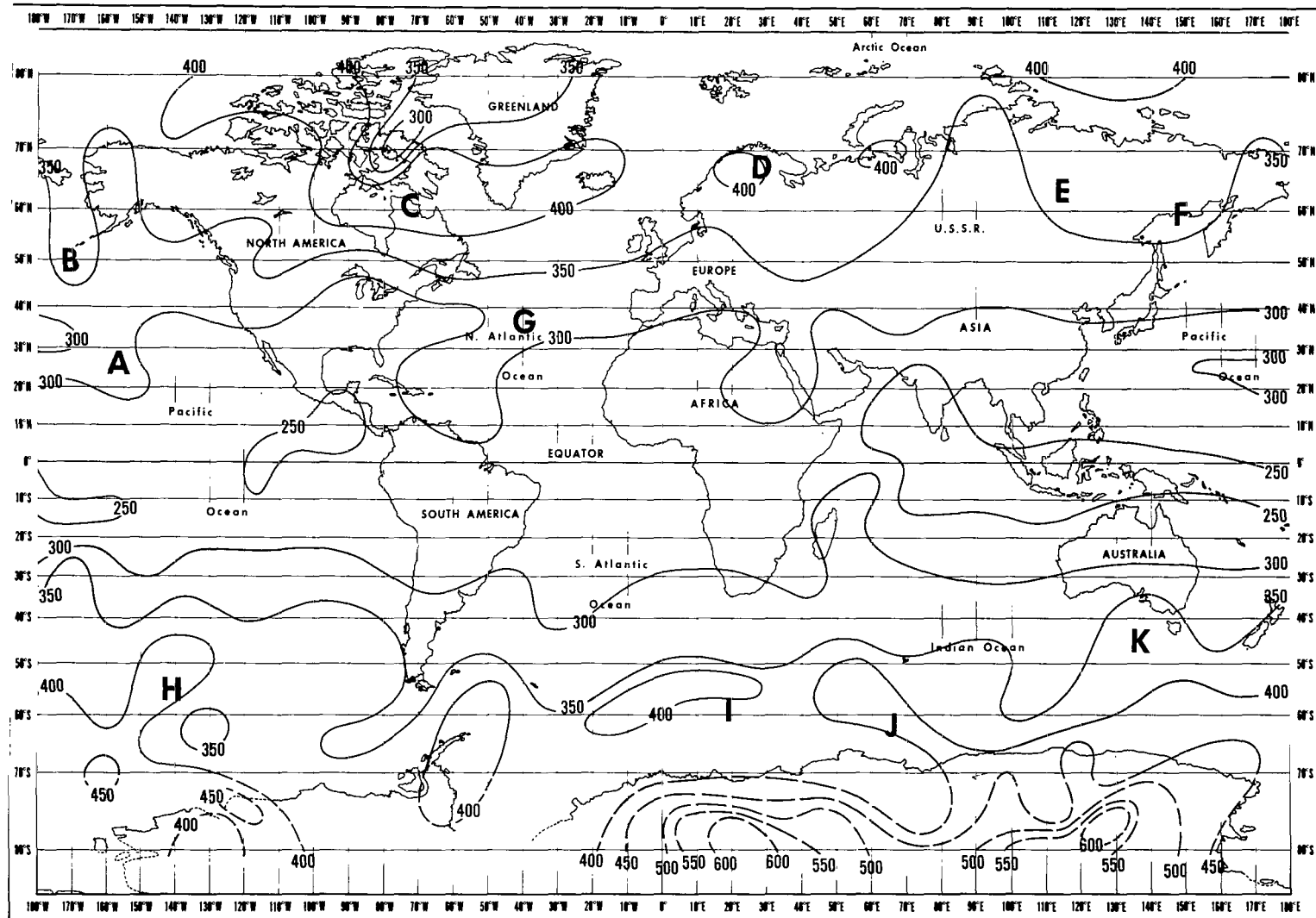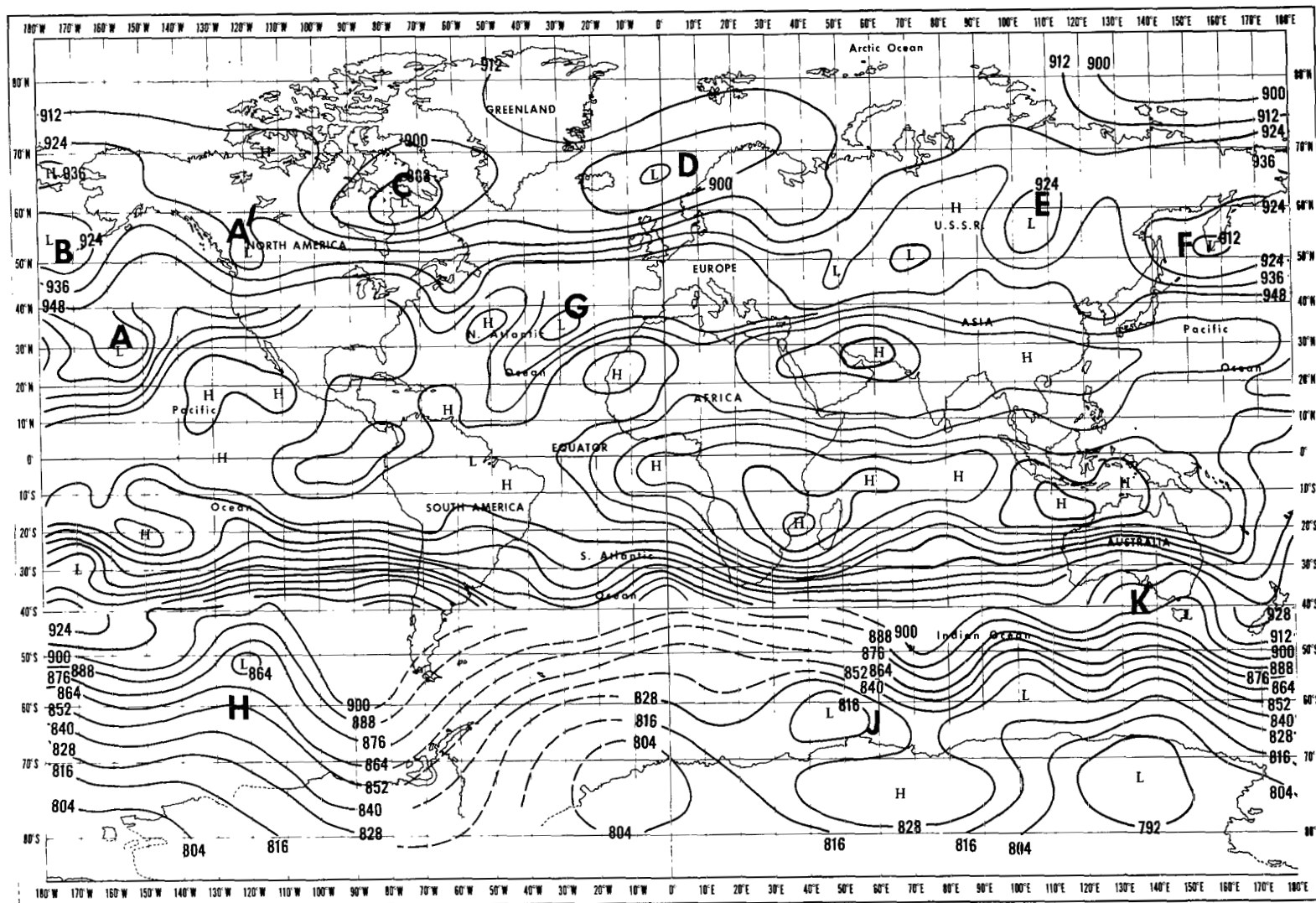
Figure 4(c)–April 24, 1969.
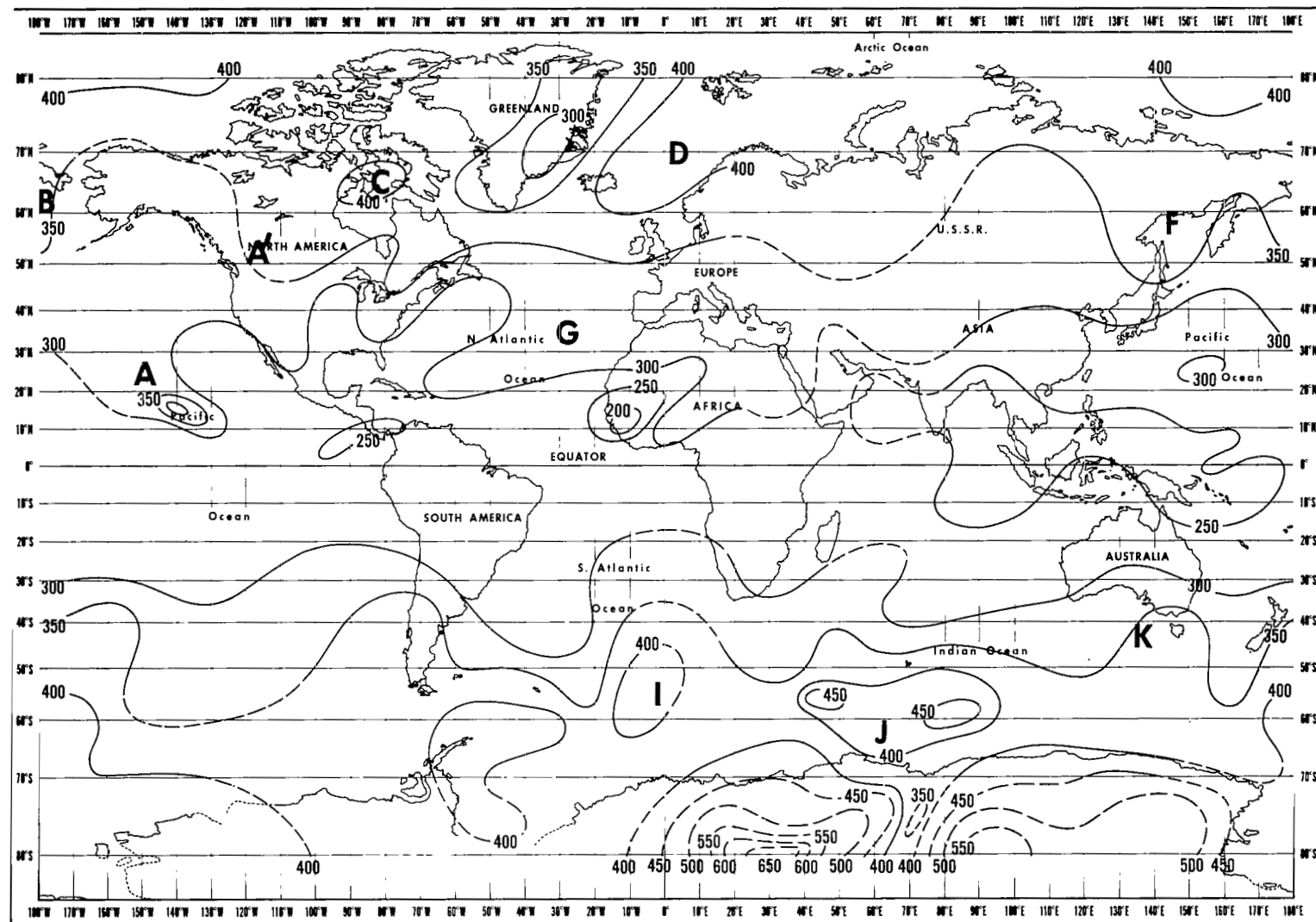
300-mb CHART, 0000 GMT

TOTAL-OZONE CONTENT (10^{-3} cm STP), NIMBUS 3 IRIS DATA

Figure 4(d)—April 25, 1969.

300-mb CHART, 0000 GMT

TOTAL-OZONE CONTENT (10^{-3} cm STP), NIMBUS 3 IRIS DATA

Figure 4(e)—April 26, 1969.

300-mb CHART, 0000 GMT

TOTAL-OZONE CONTENT (10^{-3} cm STP), NIMBUS 3 IRIS DATA
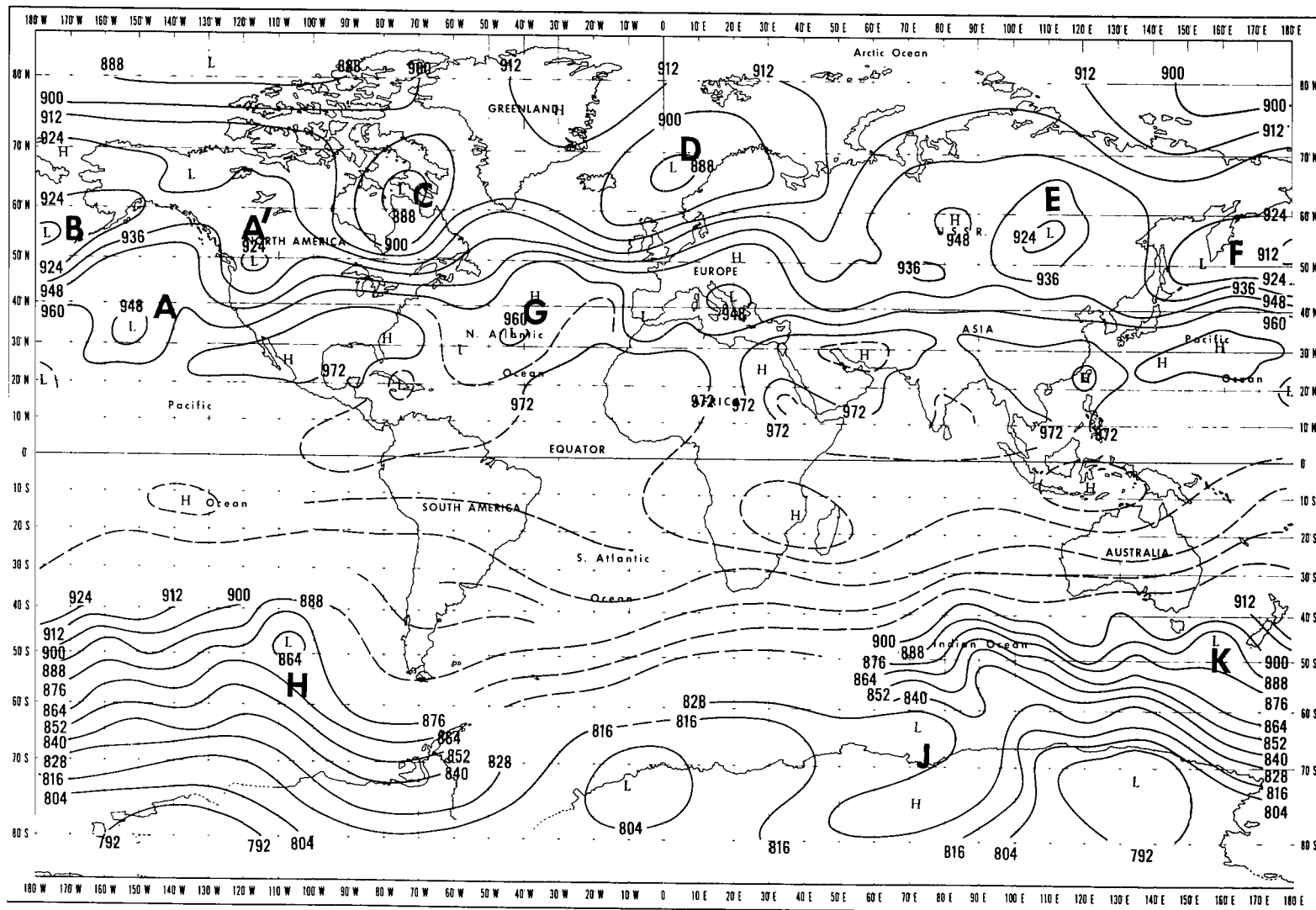
Figure 4(f)—April 27, 1969.

300-mb CHART, 0000 GMT

TOTAL-OZONE CONTENT (10^{-3} cm STP), NIMBUS 3 IRIS DATA

Figure 4(g)—April 28, 1969.

300-mb CHART, 0000 GMT

TOTAL-OZONE CONTENT (10^{-3} cm STP), NIMBUS 3 IRIS DATA
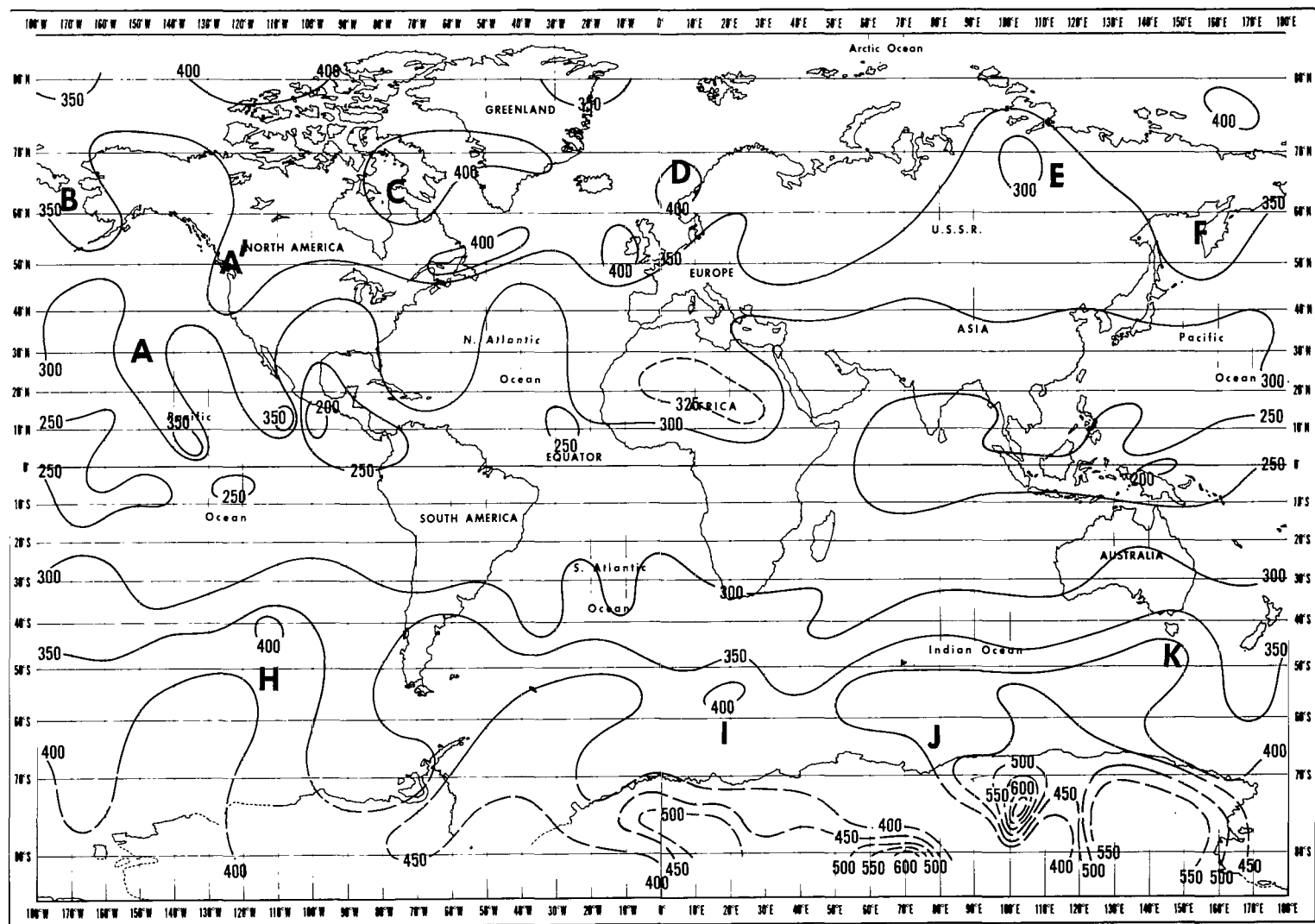
Figure 4(h)—April 29, 1969.

300-mb CHART, 0000 GMT

TOTAL-OZONE CONTENT (10^{-3} cm STP), NIMBUS 3 IRIS DATA

Figure 5(a)—July 3, 1969.

300-mb CHART, 0000 GMT

TOTAL-OZONE CONTENT (10^{-3} CM STP), NIMBUS 3 IRIS DATA

Figure 5(b)—July 4, 1969.

300-mb CHART, 0000 GMT

TOTAL-OZONE CONTENT (10^{-3} cm STP), NIMBUS 3 IRIS DATA

Figure 5(c)—July 5, 1969.

180°W 170°W 160°W 150°W 140°W 130°W 120°W 110°W 100°W 90°W 80°W 70°W 60°W 50°W 40°W 30°W 20°W 10°W 0 10°E 20°E 30°E 40°E 50°E 60°E 70°E 80°E 90°E 100°E 110°E 120°E 130°E 140°E 150°E 160°E 170°E 180°E

888 L 888 900 912 912 912 Arctic Ocean 912 900 80 N

900
912
924 H GREENLAND 900 70 N
924 L 924 D E 924 70 N
B L C 888 H 948 L 912 F
924 A' 888 948 924 L 50 N
936 NORTH AMERICA 900 H 936 936
924 L EUROPE 948 ASIA 936 924
948 948 L Pacific 948
960 948 A G 972 ASIA 960 40 N
960 N. Atlantic H H H H
972 Ocean 972 H L 30 N
972 L Pacific
972 972 972 972 972 Ocean L 20 N
EQUATOR 10 N
0
H Ocean 10 S
SOUTH AMERICA H 20 S
S. Atlantic AUSTRALIA 30 S
Ocean
924 912 900 888 912 40 S
912 L 900 Indian Ocean K 900 50 S
900 864 888 888
888 H 876 864 J 876 60 S
876 864 840 852 864
864 852 L 852
852 876 828 816 H 840 L 70 S
840 864 816 828 J 828
828 852 816 816 804 816
816 840 H L 792 816
804 828 804

792 792 804 804 816 816 804 792 80 S

180°W 170°W 160°W 150°W 140°W 130°W 120°W 110°W 100°W 90°W 80°W 70°W 60°W 50°W 40°W 30°W 20°W 10°W 0 10°E 20°E 30°E 40°E 50°E 60°E 70°E 80°E 90°E 100°E 110°E 120°E 130°E 140°E 150°E 160°E 170°E 180°E
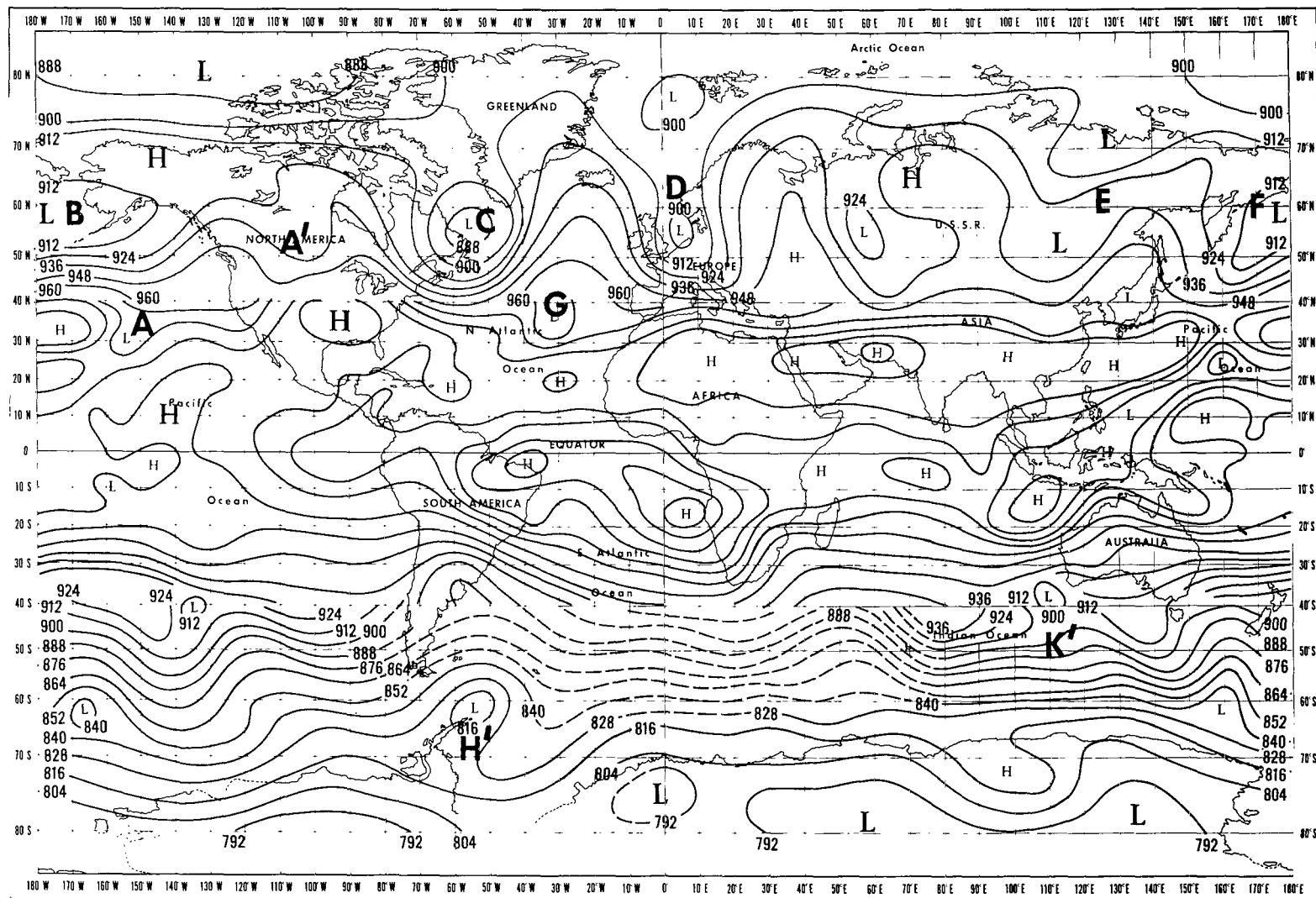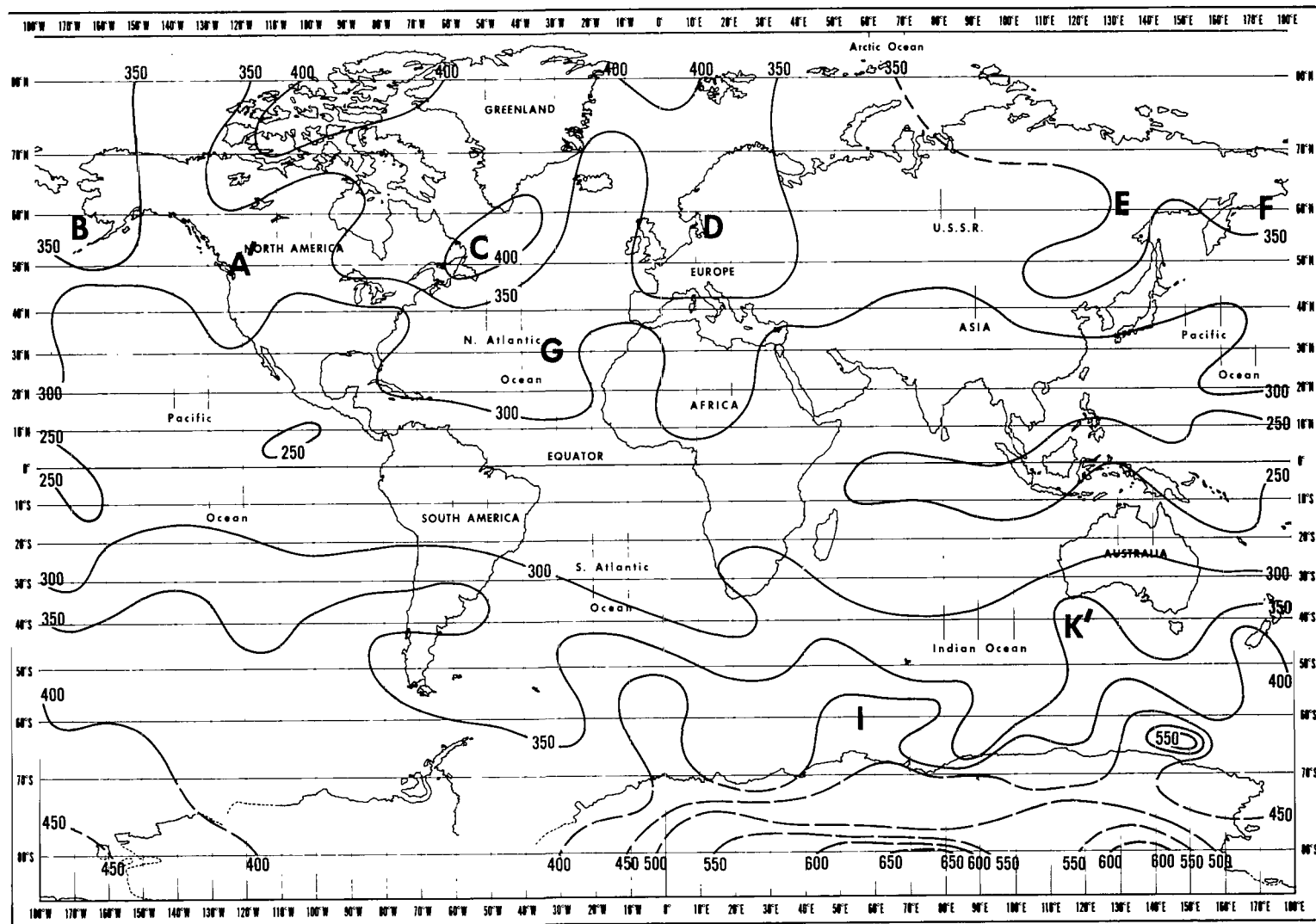
300-mb CHART, 0000 GMT

TOTAL-OZONE CONTENT (10^{-3} cm STP), NIMBUS 3 IRIS DATA
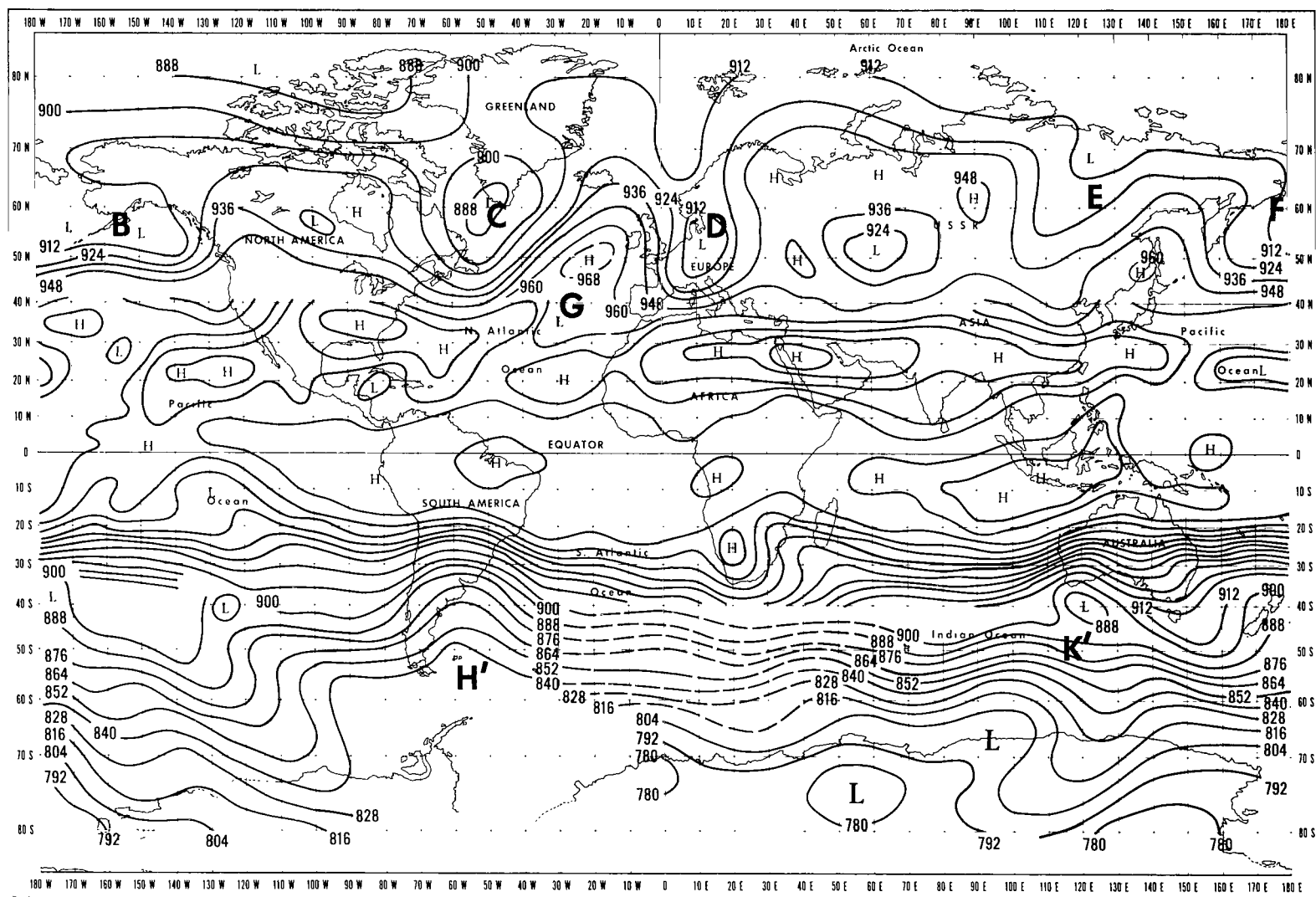
Figure 5(d)—July 6, 1969.
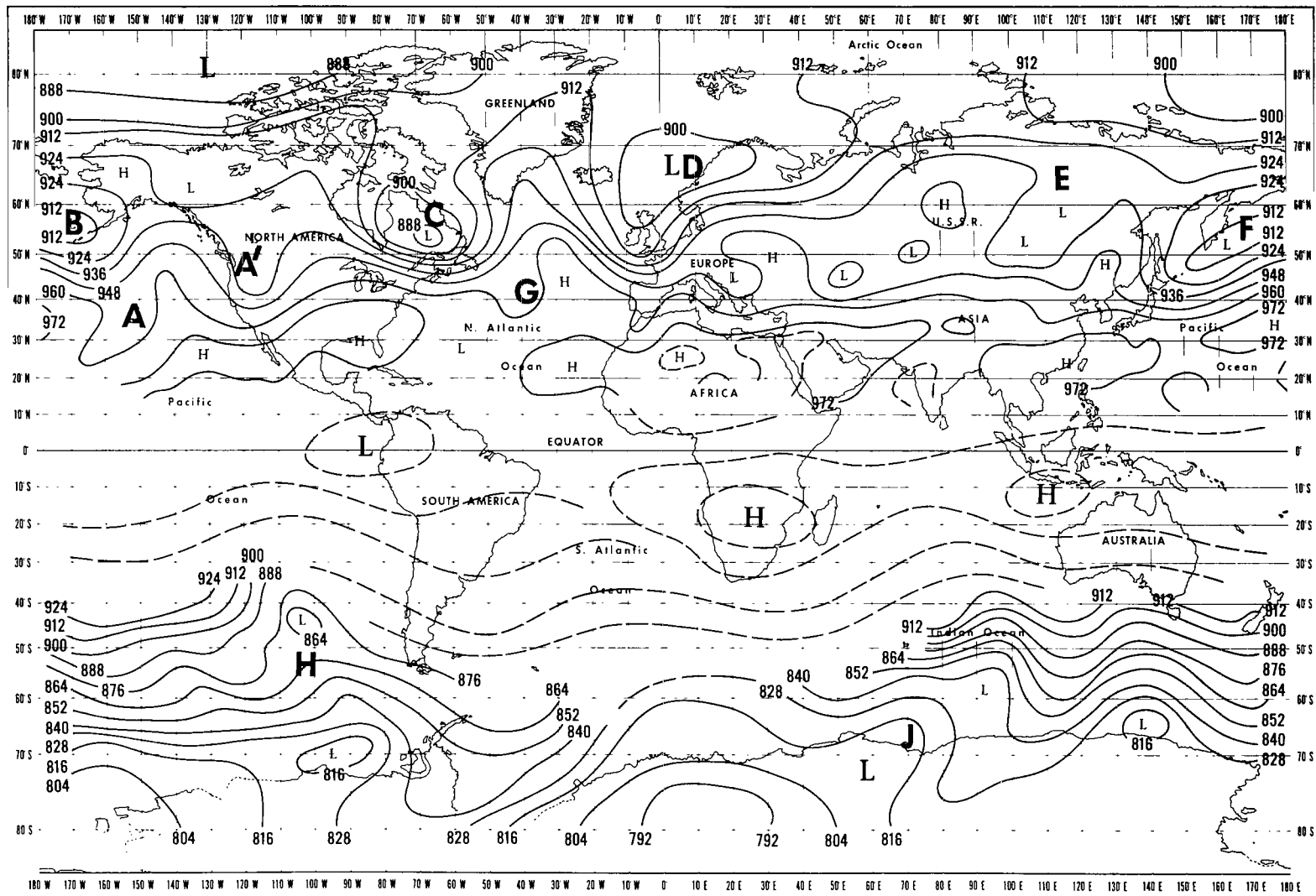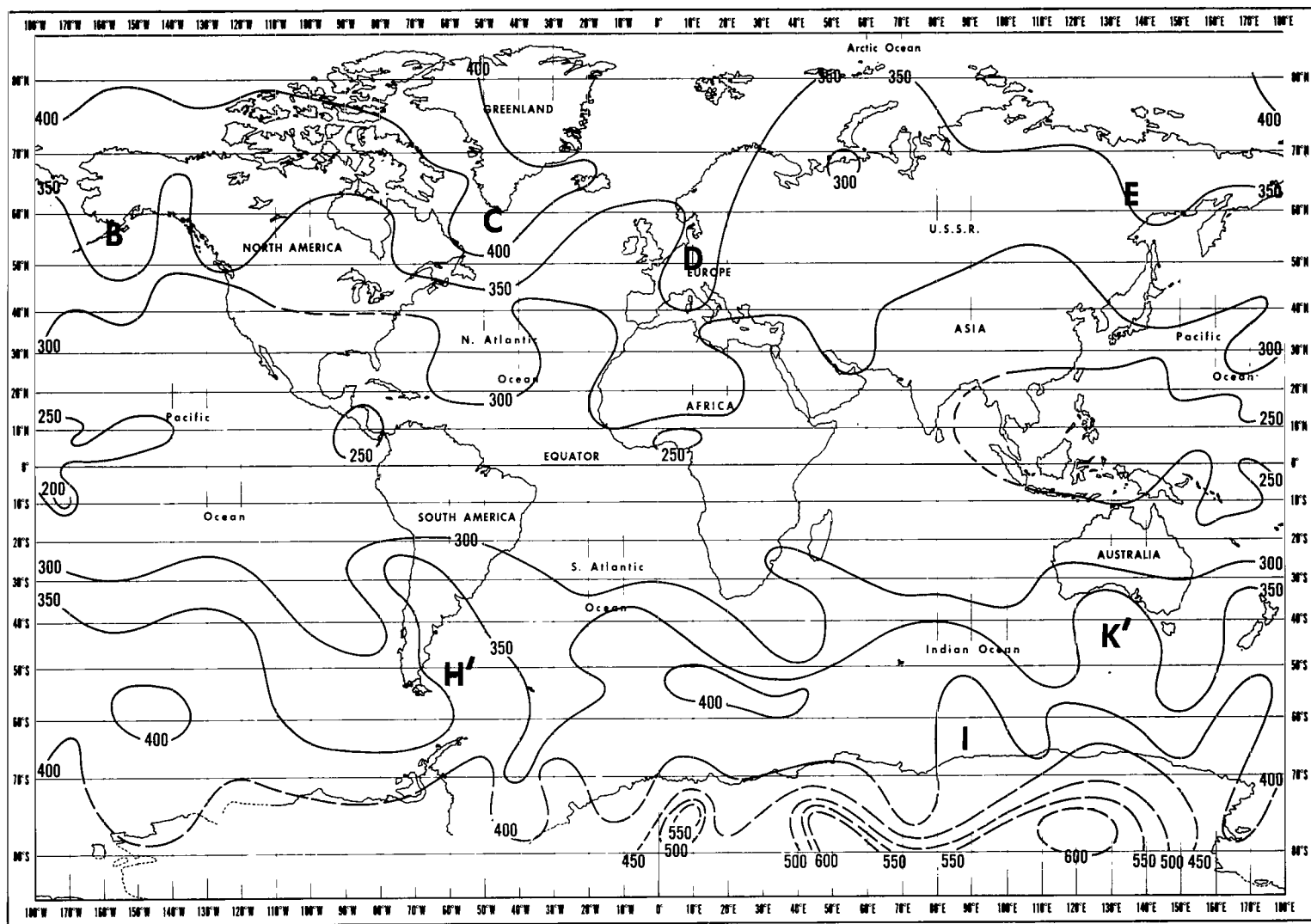
300-mb CHART, 0000 GMT
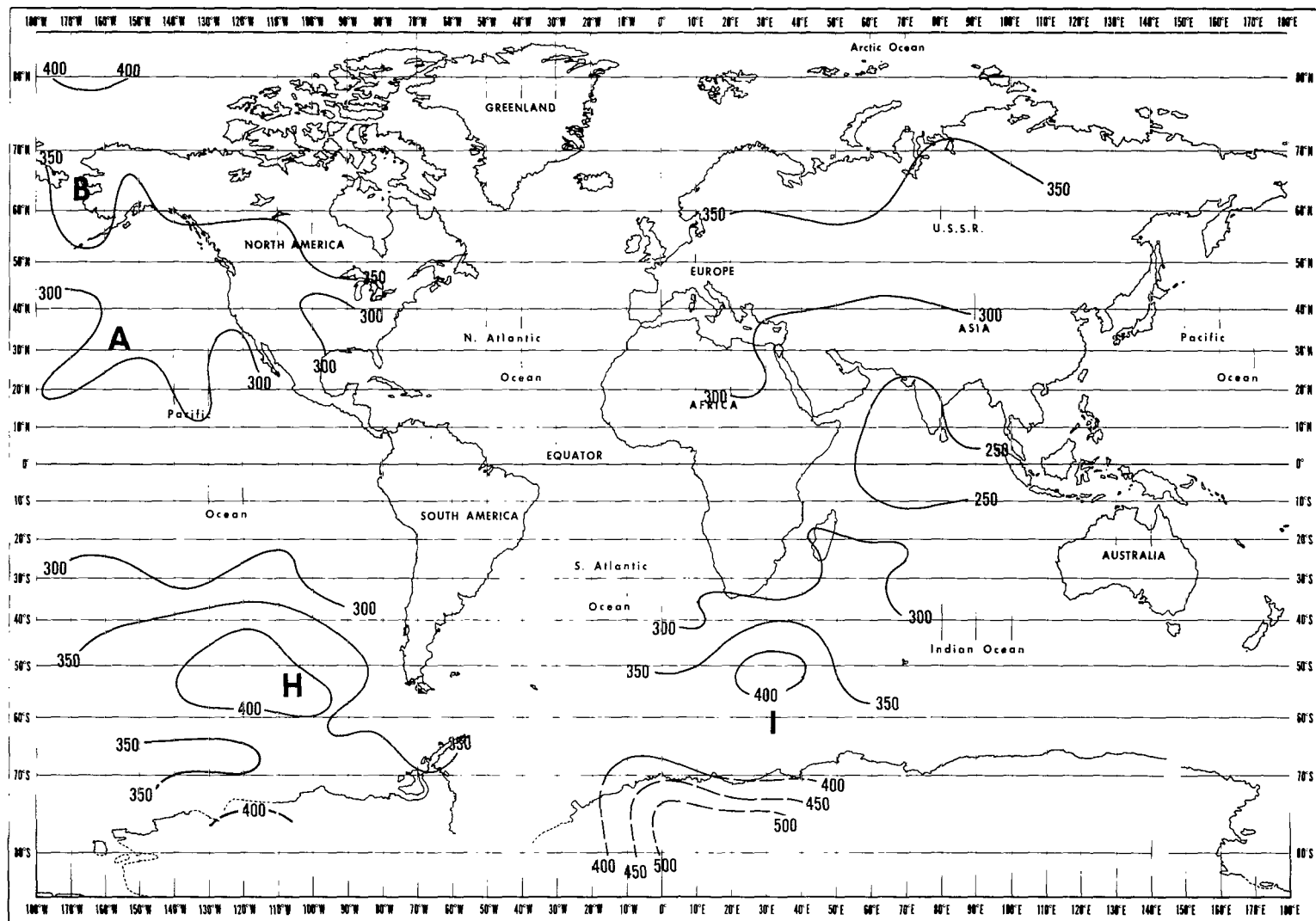
TOTAL-OZONE CONTENT (10^{-3} cm STP), NIMBUS 3 IRIS DATA
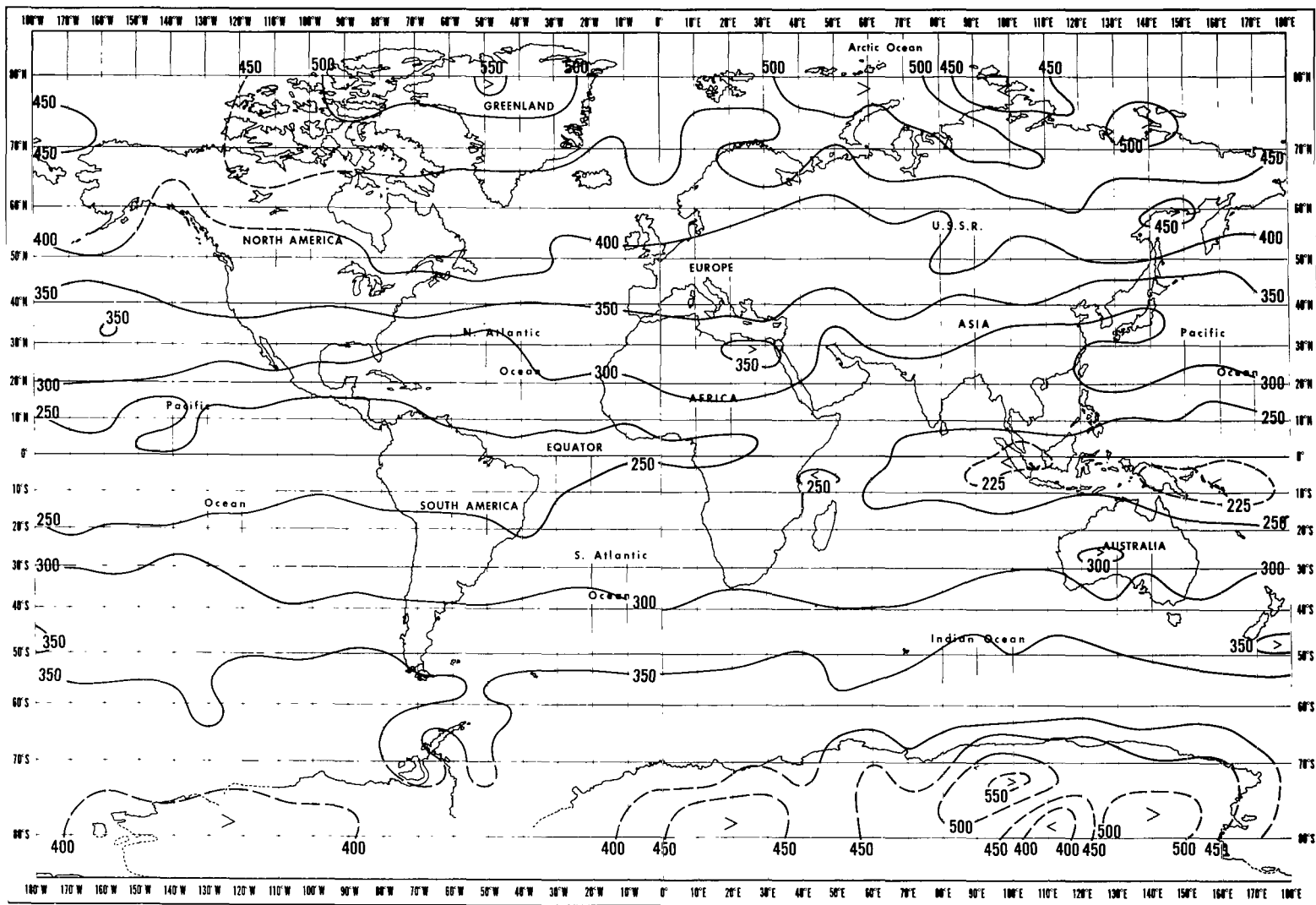
Figure 5(e)–July 7, 1969.
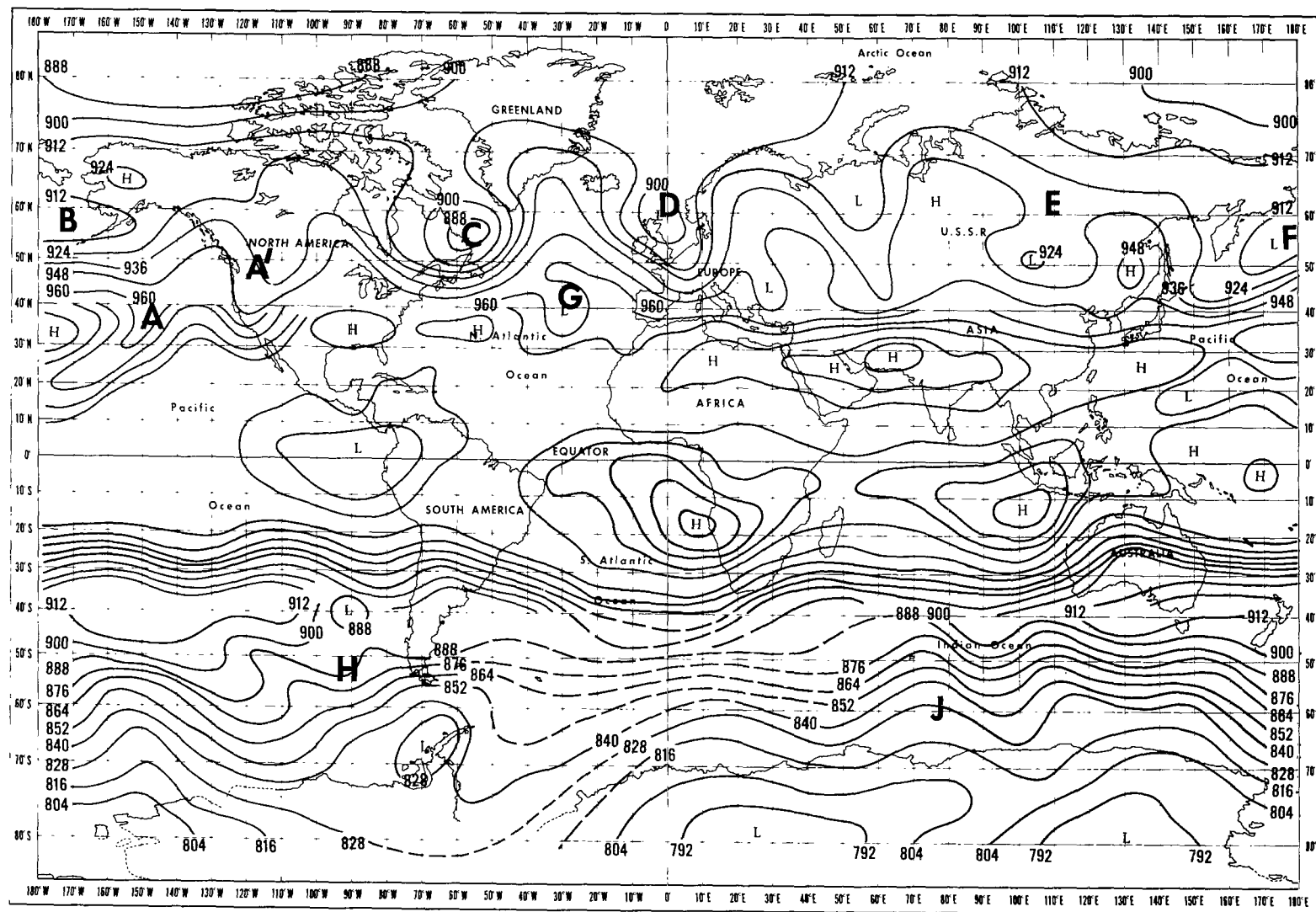
300-mb CHART, 0000 GMT
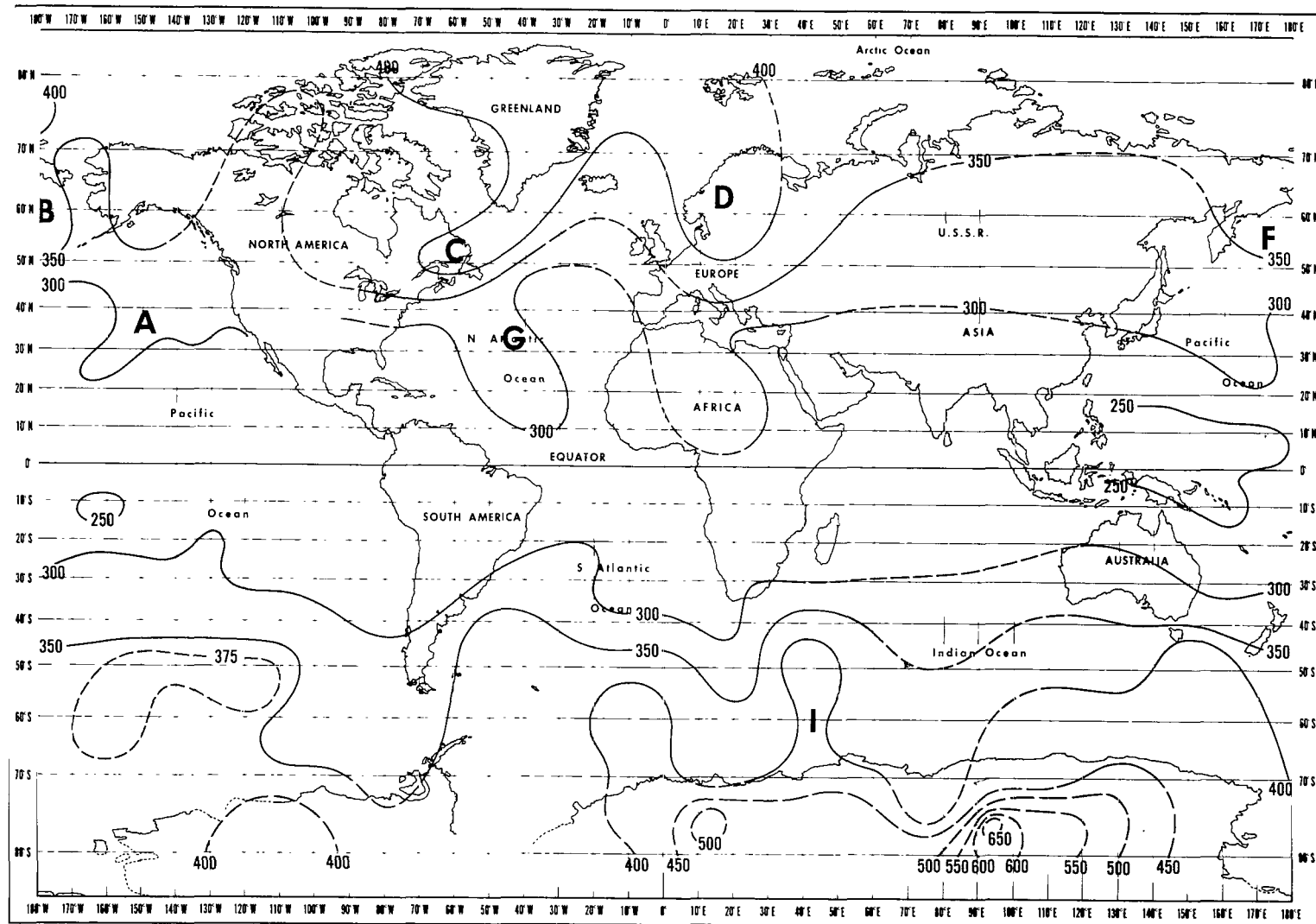
TOTAL-OZONE CONTENT (10^{-3} cm STP), NIMBUS 3 IRIS DATA

Figure 5(f)—July 8, 1969.

300-mb CHART, 0000 GMT

TOTAL-OZONE CONTENT (10^{-3} cm STP), NIMBUS 3 IRIS DATA

Figure 5(g)—July 9, 1969.

300-mb CHART, 0000 GMT

TOTAL-OZONE CONTENT (10^{-3} cm STP), NIMBUS 3 IRIS DATA

Figure 5(h)—July 10, 1969.

44

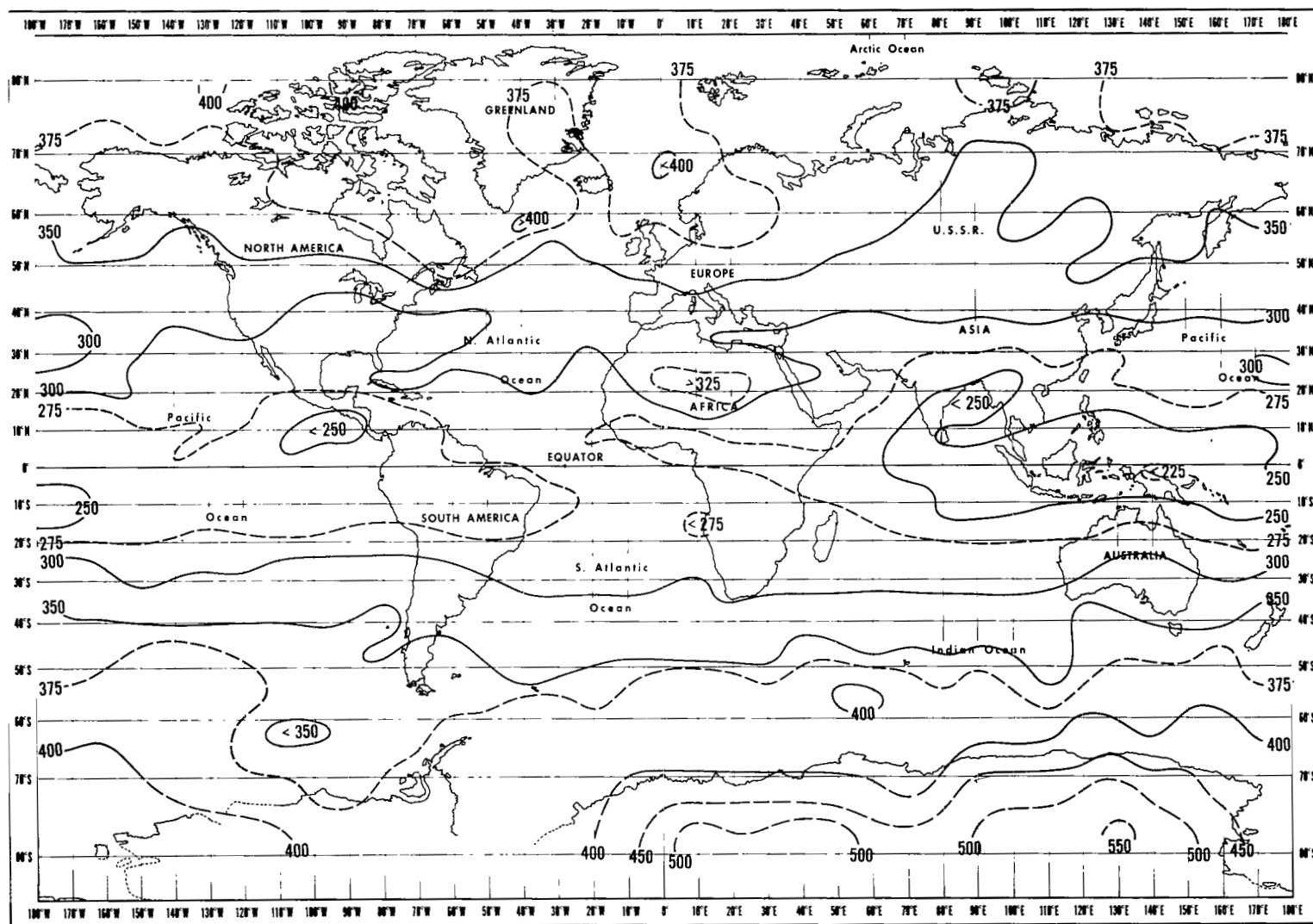Figure 6—Mean total-ozone content (10^{-3} cm STP), April 22-29, 1969, Nimbus 3 IRIS data.

Figure 7—Mean total-ozone content (10^{-3} cm STP), July 3-10, 1969, Nimbus 3 IRIS data.
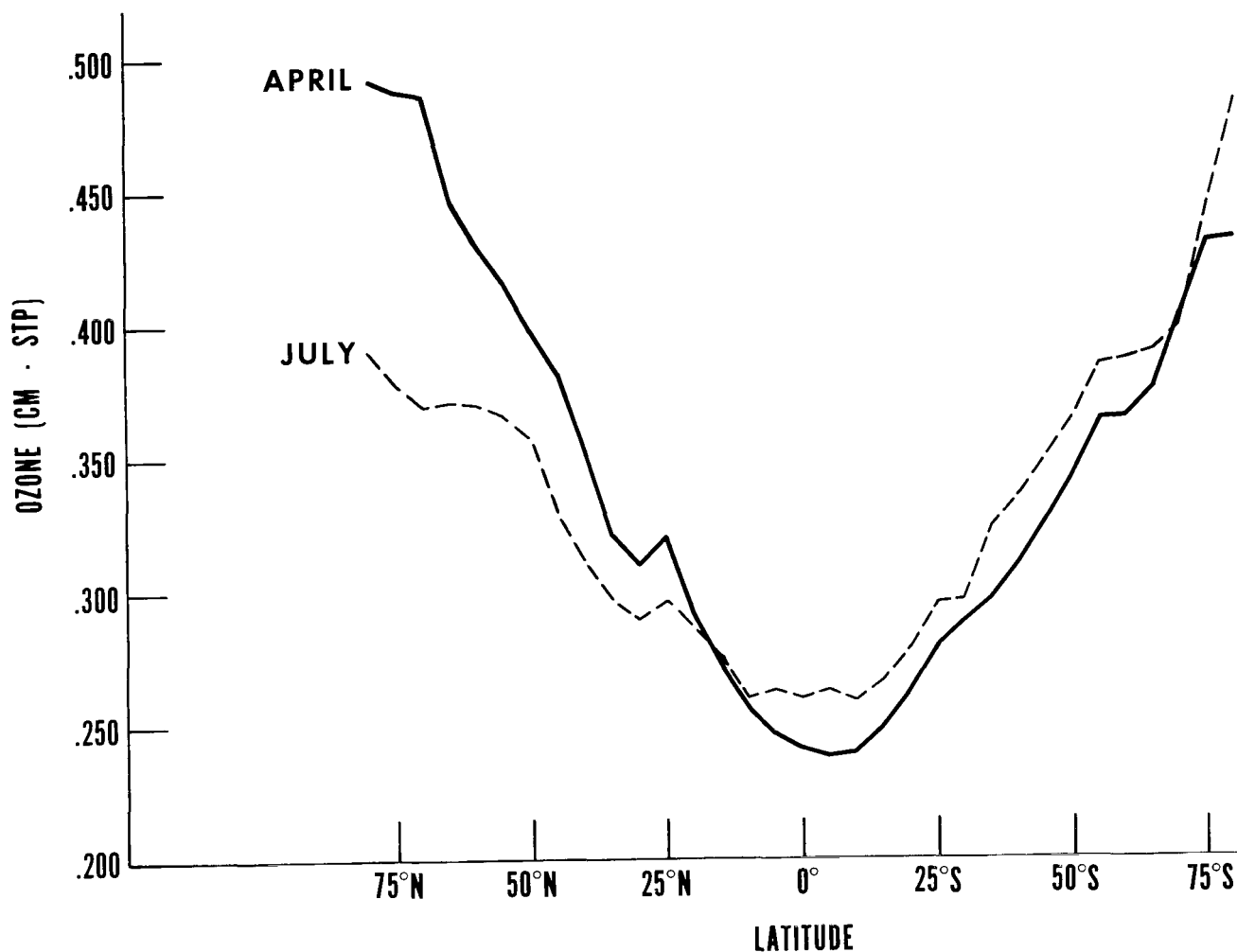
Figure 8—Latitudinal distribution of mean total-ozone content, April 22-29, 1969 and July 3-10, 1969, Nimbus 3 IRIS data.

REFERENCES

Breiland, J. G., "Variation in the Vertical Distribution of Atmospheric Ozone During the Passage of a Short Wave in the Westerlies," J. Geophys. Res., 74:4501-4510, 1969.

Brewer, A. W., and Milford, J. R., "The Oxford Kew Ozonesonde," Proc. Roy. Soc., Ser. A, 256:470-495, 1960.

Chapman, S., "A Theory of Upper Atmospheric Ozone," Memoirs, Roy. Meteorol. Soc., 3:103, 1930.

Conrath, B., Hanel, R., Kunde, V., and Prabhakara, C., "The Infrared Interferometer Experiment on Nimbus 3," J. Geophys. Res., 75(30):5831-5857, 1970.

Craig, R. A., "The Observations and Photochemistry of Atmospheric Ozone and their Meteorological Significance," Meteorological Monographs, Vol. 1, No. 2, American Meteorological Society, Boston, Mass., 1950, p. 50.

Danielson, E. F., "Stratospheric-Tropospheric Exchange Based on Radioactivity, Ozone and Potential Vorticity," J. Atmos. Sci., 25:502-518, 1968.

Dave, J. V., Sheppard, P. A., and Walshaw, C. D., "Ozone Distribution and the Continuum from Observations in the Region of the 1,043 cm^{-1} Band," Quart. J. Roy. Meteorol. Soc., 89(381):307-318, 1963.

Dobson, G. M. B., Harrison, D. N., and Lawrence, J., "Measurements of the Amount of Ozone in the Earth's Atmosphere and Its Relation to Other Geophysical Conditions," Proc. Roy. Soc., Ser. A, 114:521-541, 1927.

Dobson, G. M. B., "A Photoelectric Spectrometer for Measuring the Amount of Atmospheric Ozone," Proc. Phys. Soc., London, 43:324-339, 1931.

Dütsch, H. V., "Atmospheric Ozone and Ultraviolet Radiation" in "Climate of the Free Atmosphere," World Survey of Climatology, Vol. 4, New York: Elsevier, 1969, pp. 383-432.

Epstein, E. S., Oesterberg, C. H., and Adel, A., "A New Method for Determination of Ozone from a Ground Station," J. Meteorol., 13:319-334, 1956.

Freie Universität, Berlin, Institut für Meteorologie und Geophysik, Meteorologische Abhandlungen, 93(4), April 1969; 94(7), July 1969.

Gotz, F. W. P., Meetham, A. R., and Dobson, G. M. B., "The Vertical Distribution of Ozone in the Atmosphere," Proc. Roy. Soc., Ser. A, 145:416-446, 1934.

Griggs, M., "Atmospheric Ozone: The Middle Ultraviolet, Its Science and Technology," Chapter 4, Atmospheric Ozone (ed. by A. E. S. Green), New York: John Wiley and Sons, Inc., 1966, pp. 83-117.

Hampson, J., "Photochemical Behavior of the Ozone Layer," Technical Note 1627/64, Canadian Armaments Research and Development Establishment, Valcartier, Quebec, 1964, p. 280.

Hering, W. S., and Borden, T. R., Jr., "Ozone Observations Over North America," Vol. 3, AFCRL-64-30(III), Environmental Research Paper No. 133, Air Force Cambridge Research Laboratories, Bedford, Mass., 1965.

Hering, W. S., and Borden, T. R., Jr., "Ozone Observations Over North America," Vol. 4, AFCRL-64-30(IV), Environmental Research Paper No. 279, Air Force Cambridge Research Laboratories, Bedford, Mass., 1967.

Hilsenrath, E., Seiden, L., and Goodman, P., "An Ozone Measurement in the Mesosphere and Stratosphere by Means of a Rocketsonde," J. Geophys. Res., 74: 6873-6880, 1969.

Holmstrom, I., "On a Method for Parametric Representation of the State of the Atmosphere," Tellus, 15(2):127-149, 1963.

Hunt, B. G., "Photochemistry of Ozone in the Moist Atmosphere," J. Geophys. Res., 71:1385-1398, 1966.

Iozenas, U. A., Krasnopol'skiy, V. A., Kuznetzov, A. P., and Lebedinskiy, A. I., "An Investigation of the Planetary Ozone Distribution from Satellite Measurements of Ultraviolet Spectra," Izv. Acad. Sci. USSR, Atmos. Oceanic Phys., 5(4):395-403, 1969.

Junge, C. E., "Global Ozone Budget and Exchange Between Stratosphere and Tropopause," Tellus, 14(4):363-377, 1962.

Komhyr, W. D., "A Carbon-Iodine Ozone Sensor for Atmospheric Sounding" in "Proceedings of the Ozone Symposium," Albuquerque, N.M., 1964, World Meteorol. Assn., Geneva, Switz., 1965, p. 26.

Komhyr, W. D., and Sticksel, P. R., "Ozonesonde Observations 1962-1966," IER 51-IAS1, Institutes for Environmental Research, ESSA, Boulder, Colo., 1967, pp. 328.

Krueger, A., "Rocket Measurements of Ozone in Hawaii," Ann. Geophys., 25:307-311, 1969.

Leovy, C., "Atmospheric Ozone: An Analytical Model for Photochemistry in the Presence of Water Vapor," J. Geophys. Res., 74:417-426, 1969.

London, J., Ooyama, K., and Prabhakara, C., "Mesosphere Dynamics," AFCRL 62-672, Contract No. AF 19(604)-5492, New York University, New York, N. Y., 1962, pp. 109.

Meetham, A. R., "The Correlation of the Amount of Ozone with the Other Characteristics of the Atmosphere," Quart. J. Roy. Meteorol. Soc., 63:289-307, 1937.

Nagata, T., Tohmatsu, T., and Tsuruta, H., "Observations of Mesospheric Ozone Density in Japan," Space Research VIII, Amsterdam: North-Holland Publishing Co., 1967, pp. 639-646.

Newell, R. E., "Stratospheric Energetics and Mass Transport," Pure and Appl. Geophys., 58:145-156, 1964.

NOAA, "Upper Air Tropical Stream Function Charts," National Meteorological Center, Washington, D. C., 1969.

Paetzold, H. K., "Die Vertikale Verteilung des Atmospharischen Ozons Nach den Photochemischen Gleichgewicht", Geofis. Pura Appl., 24:1-14, 1953.

Paetzold, H. K., and Regener, E., "Ozon in der Erdatmospare," Handbook der Physik, 48, Geophysik II (ed. by S. Flugge), Berlin: Springer Verlag, 1957, pp. 370-426.

Peng, L., "A Simple Numerical Experiment Concerning the General Circulation in the Lower Stratosphere," Pure and Appl. Geophys., 61:191-218, 1965.

Plass, G. N., "Models for Spectral Band Absorption," J. Opt. Soc. Am., 48(10):690-703, 1958.

Prabhakara, C., "Feasibility of Determining Atmospheric Ozone from Outgoing Infrared Energy," Mon. Weather Rev., 97(4):307-314, 1969.

Prabhakara, C., Conrath, B. J., and Hanel, R. A., "Remote Sensing of Atmospheric Ozone Using the 9.6μ Band," J. Atmos. Sci., 27(4):689-697, 1970.

Ramanatham, K. R., "Atmospheric Ozone and the General Circulation of the Atmosphere," in Scientific Proc. of the Int. Ass. of Met., Rome, 1954, London: Butterworth Scientific Publications, 1954, pp. 3-24.

Randhawa, J., "Ozonesonde for Rocket Flight," Nature, 213:53-54, 1967.

Rawcliffe, R. D., Meloy, G. E., Friedman, R. M., and Rogers, E. H., "Measurement of Vertical Distribution of Ozone from a Polar Orbiting Satellite," J. Geophys. Res., 68(24):6425-6429, 1963.

Regener, V. H., "Vertical Flux of Atmospheric Ozone," J. Geophys. Res., 62:221-228, 1957.

Regener, V. H., "On a Sensitive Method for Recording of Atmospheric Ozone," J. Geophys. Res., 65:3975-3977, 1964.

U. S. Navy, "Southern Hemisphere Upper Air Charts," McMurdo Station, Antarctica, 1969. Available from Bldg. R-48, U. S. Navy Weather Research Facility, Norfolk, Va.

Appendix A

Atmospheric-Temperature Soundings

IRIS spectral measurements are first inverted to give the atmospheric-temperature distribution, and the ozone-inversion scheme is used subsequently. Although the atmospheric-temperature soundings have been obtained for the maps of April 22-30 and July 3-10, 1969, this information has not yet been described in this study. This appendix will present temperature maps for the 50-mb and 10-mb levels for five days in April (25-29), 1969 (Figures A-1 to A-5).

Each figure includes a 50-mb map (a) and a 10-mb map (b). Areas having temperatures below 213 K are shaded to aid the description. The temperature maps of the stratospheric levels have been presented because these levels are least affected by the tropospheric clouds. Furthermore, the total-ozone maps depend significantly on this stratospheric-temperature data.

The 50-mb (approximately 21 km) maps reflect the lower stratospheric regimes. In the middle and high latitudes of the northern hemisphere the dominant character of about four or five of the long waves can be noticed, with the travelling short waves superimposed upon them. The tropical regions between 20°N and 20°S form a transition area between northern and southern hemisphere. The temperatures, in general, increase from equator (approximately 208 K) to pole (approximately 228 K) in the northern hemisphere during April. This is not so in the southern hemisphere, as there is a large cold pool of air present over Antarctica. The lower stratosphere of the southern hemisphere thus appears to be dominated by wave number regimes of 1 and probably also 2.

The 10-mb (approximately 32 km) level maps show primarily the increase of temperature from south pole (208 K) to north pole (235 K). Wave numbers 1 and 2 contain most of the energy on a global scale. This seems to suggest the significant transition from the lower stratosphere (50-mb), to upper stratosphere (10-mb). The isotherms south of about 30°S show a tight, nearly circumpolar, gradient in temperature. On the contrary, north of that latitude, including most of the tropics, the temperature gradients have significantly weakened, leading to the development of large-amplitude (north-south) waves.
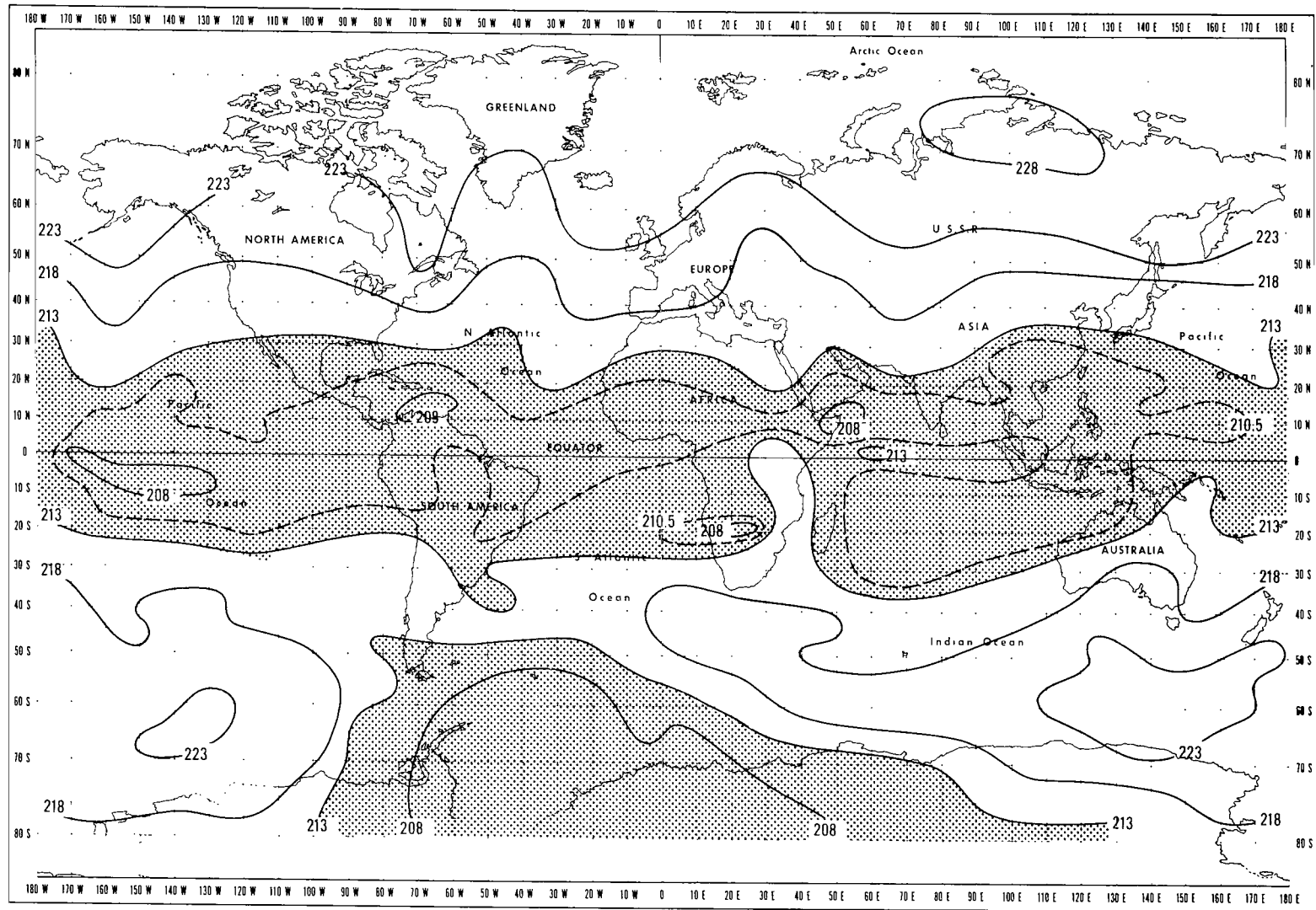
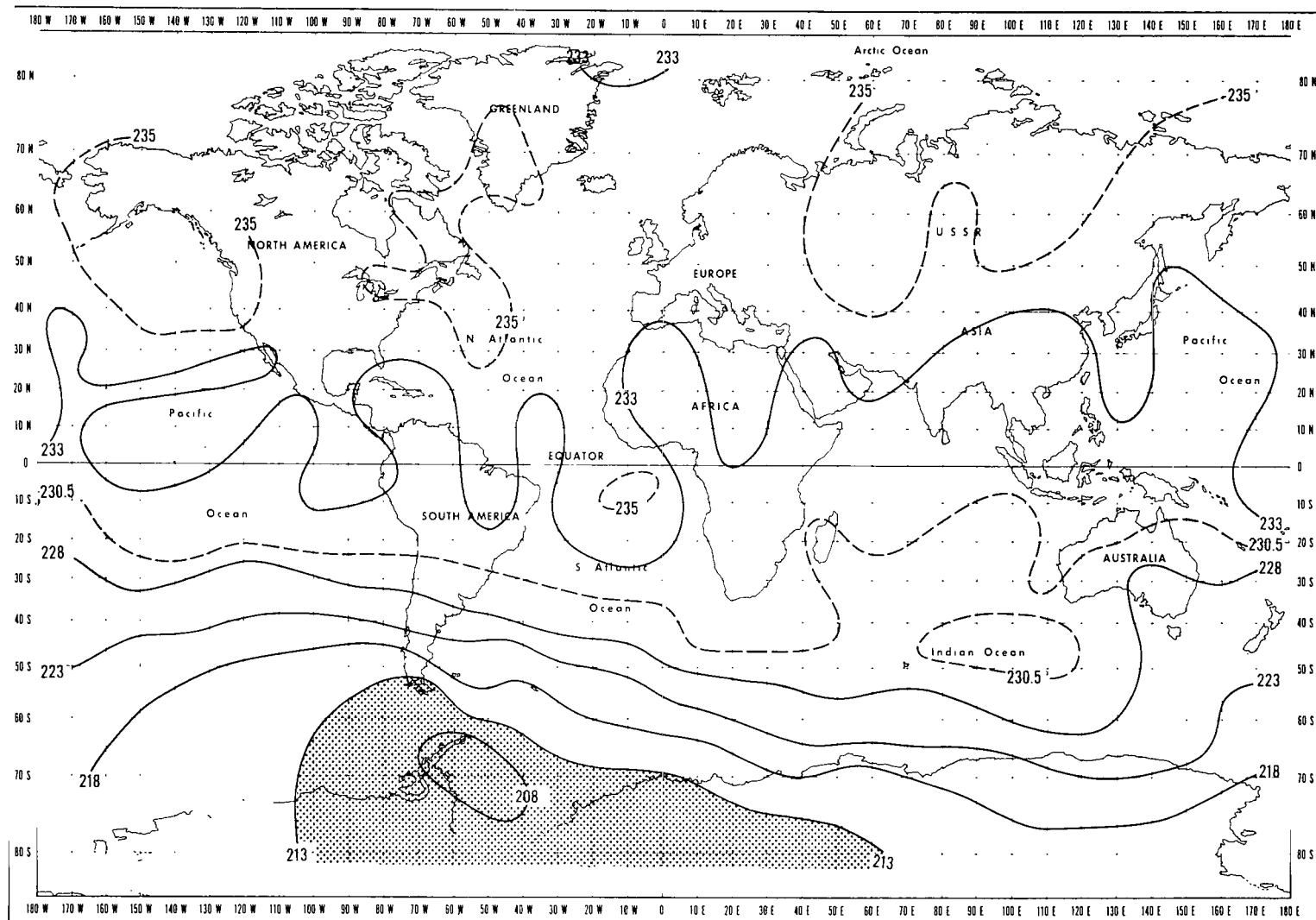Figure A-1(a)—50-mb temperatures (K) Nimbus 3 IRIS data, April 25, 1969.

Figure A-1(b)—10-mb temperatures (K), Nimbus 3 IRIS data, April 25, 1969.
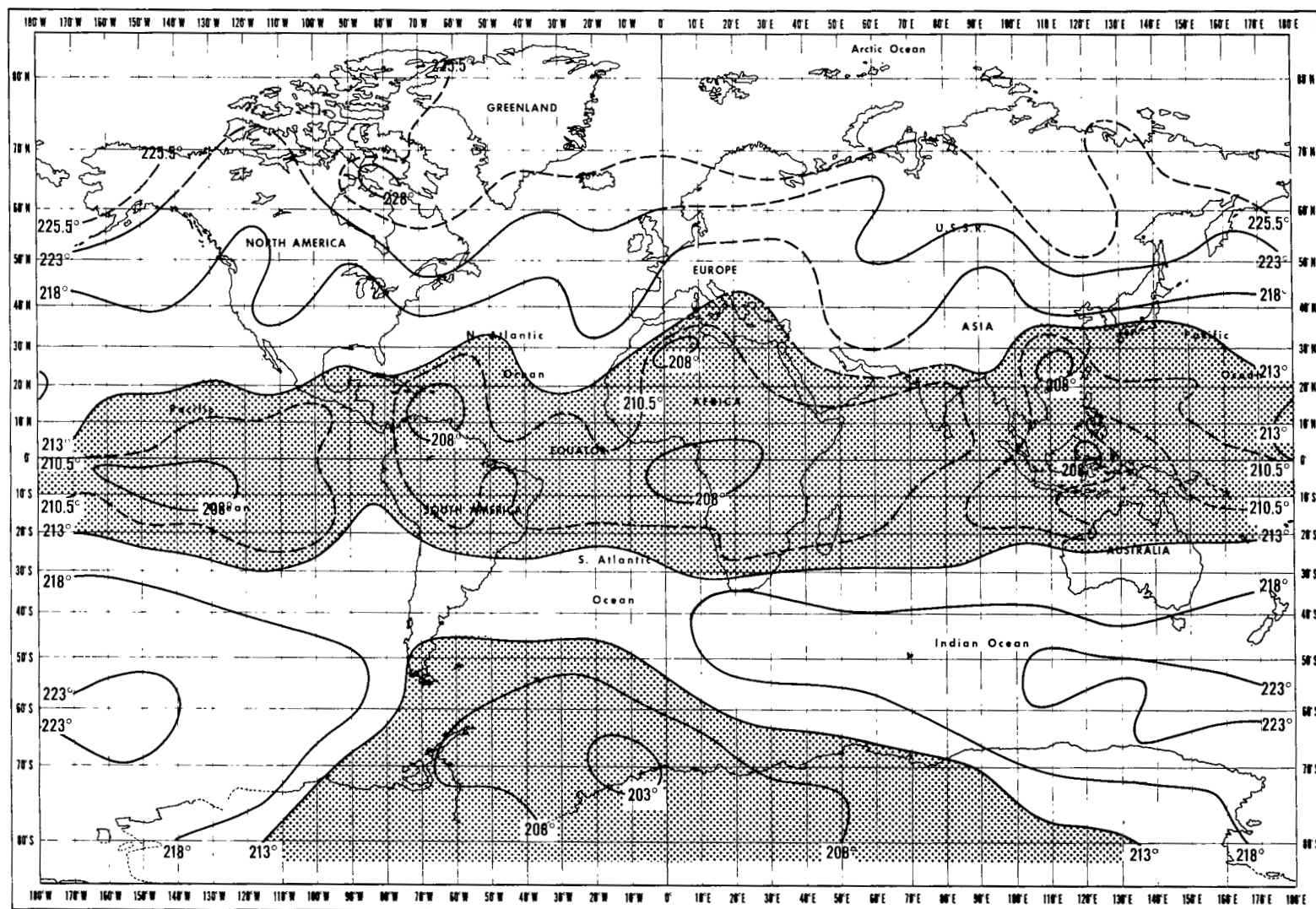
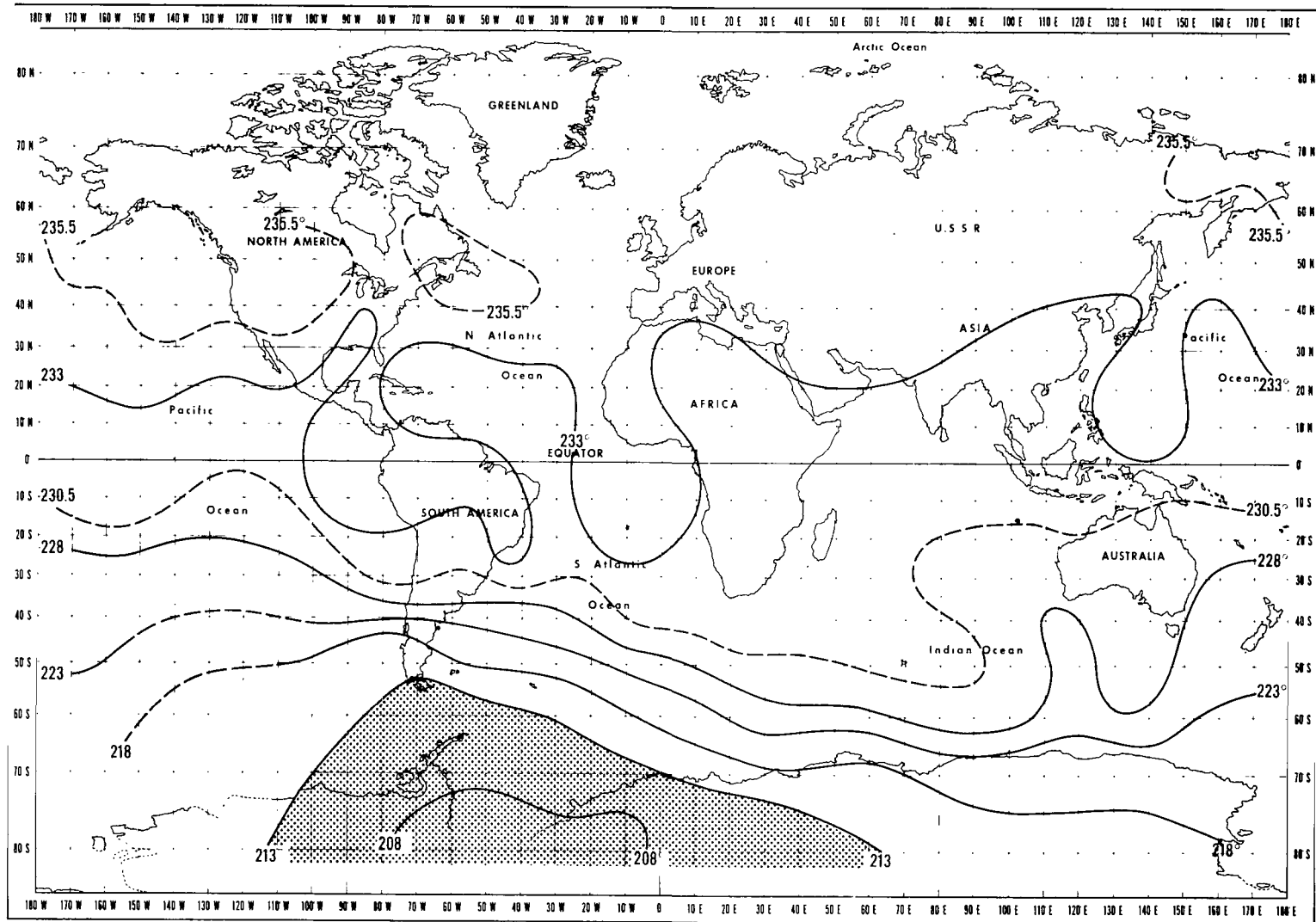Figure A-2(a)—50-mb temperatures (K), Nimbus 3 IRIS data, April 26, 1969.

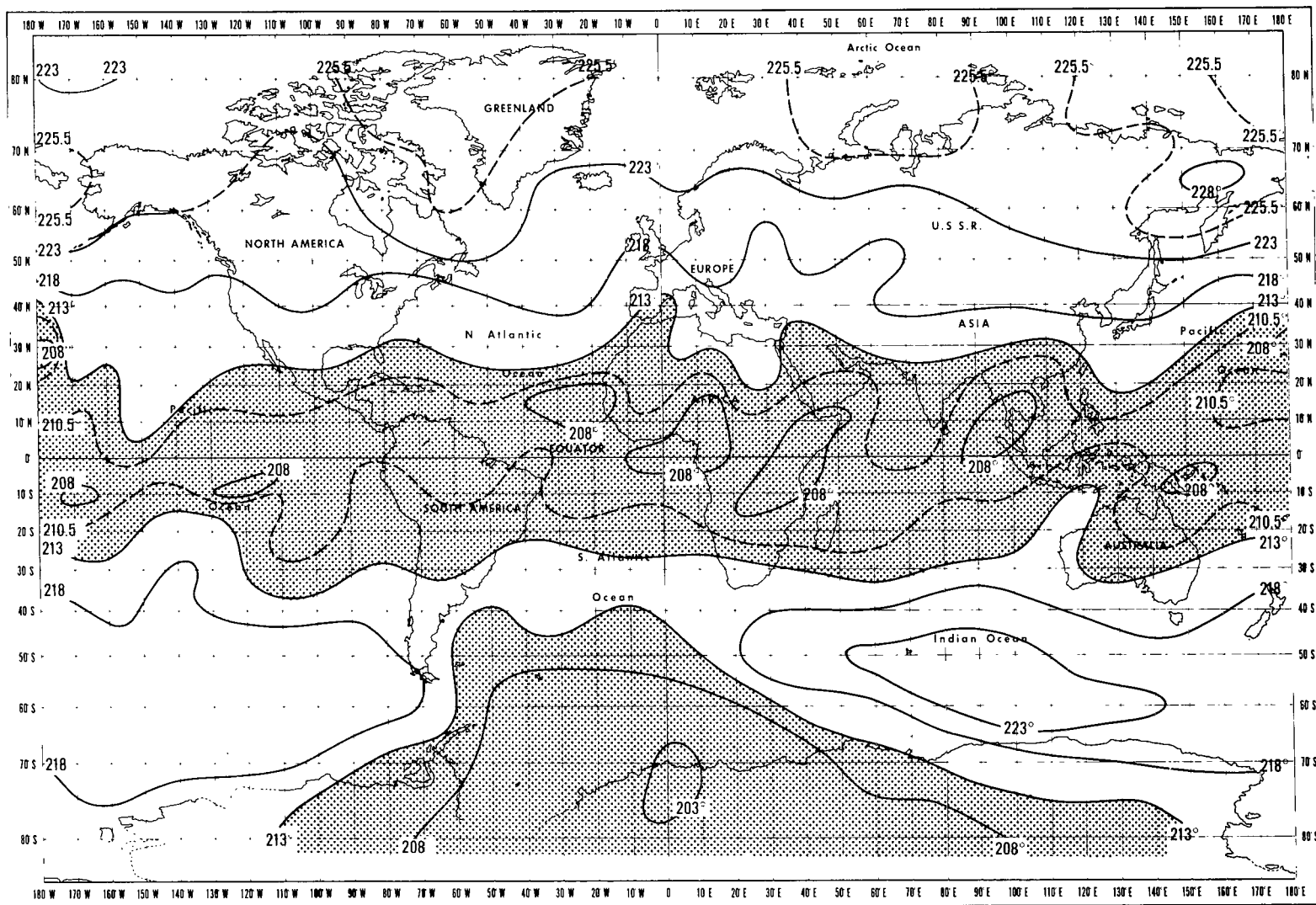Figure A-2(b)—10-mb temperatures (K), Nimbus 3 IRIS data, April 26, 1969.

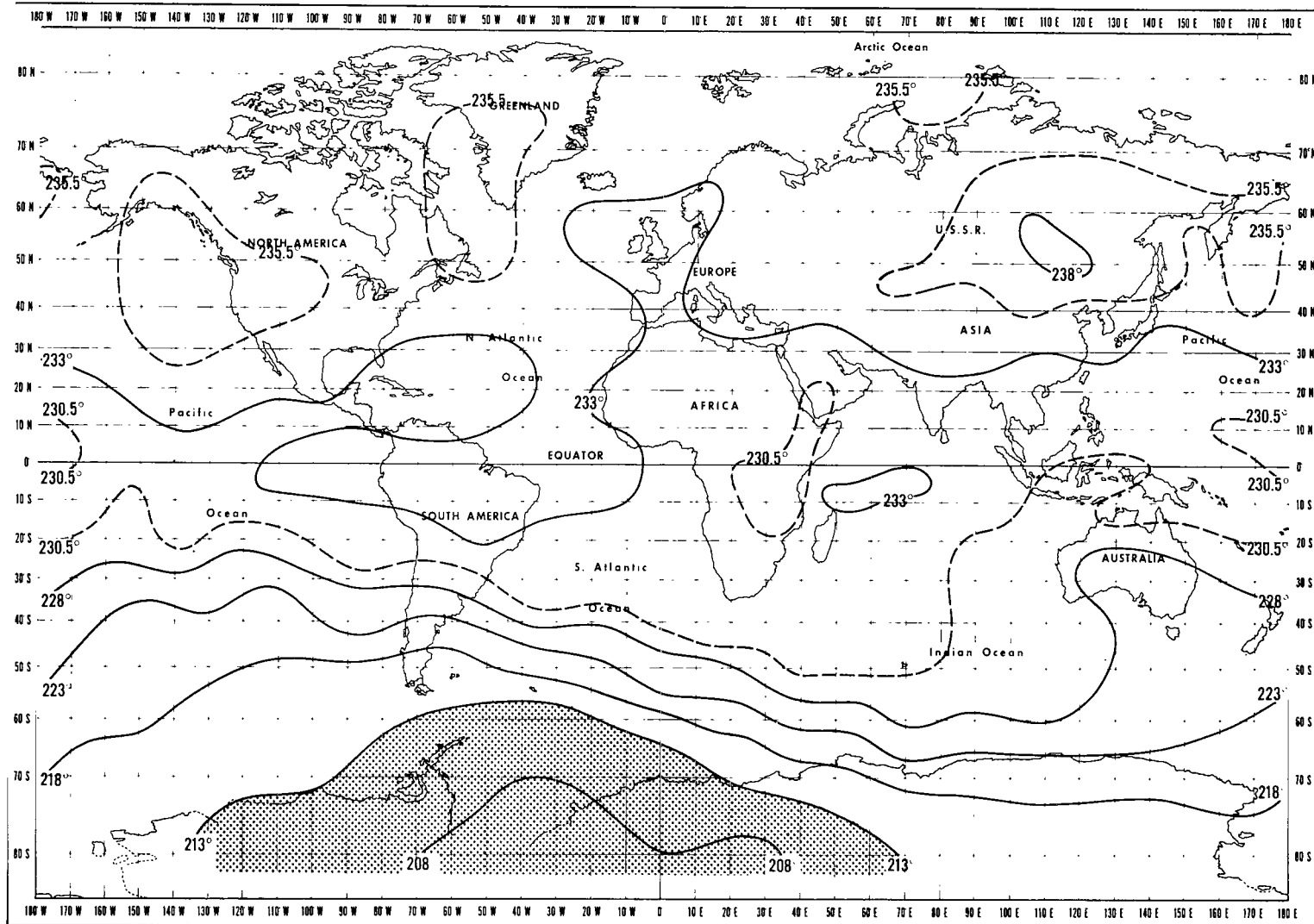Figure A-3(a)—50-mb temperatures (K), Nimbus 3 IRIS Data, April 27, 1969.

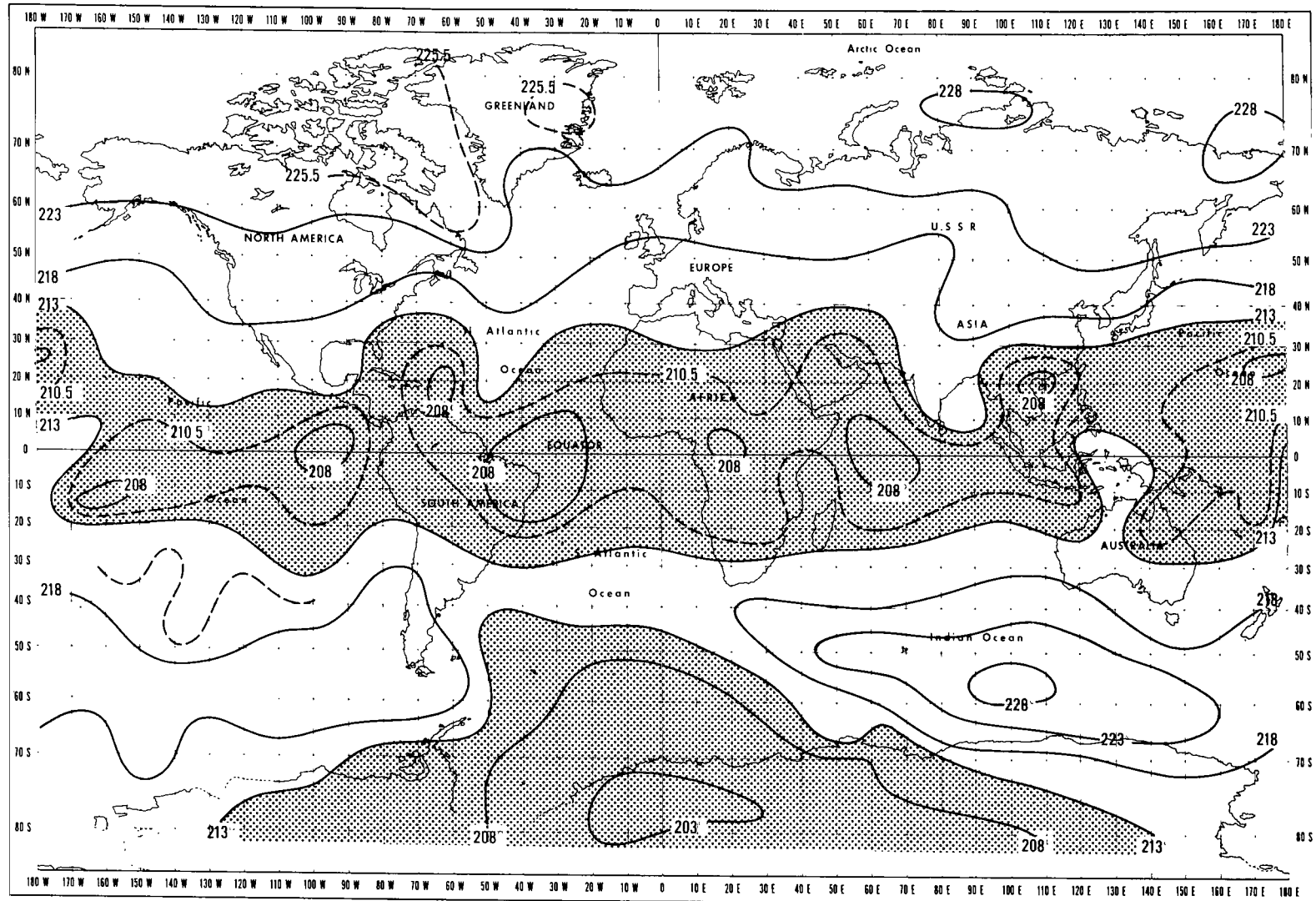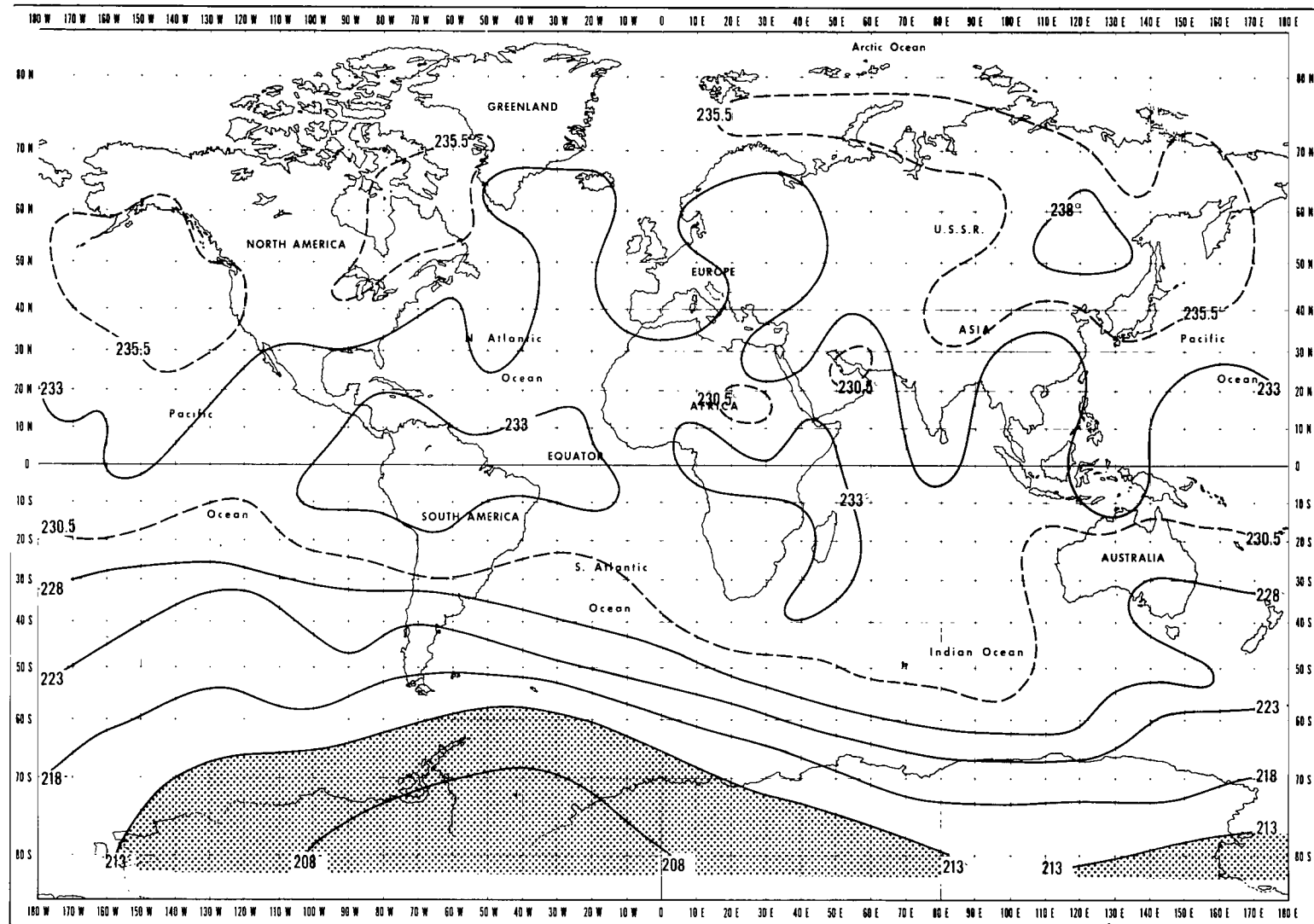Figure A-3(b)—10-mb temperatures (K), Nimbus 3 IRIS data, April 27, 1969.

Figure A-4(a)—50-mb temperatures (K), Nimbus 3 IRIS data, April 28, 1969.

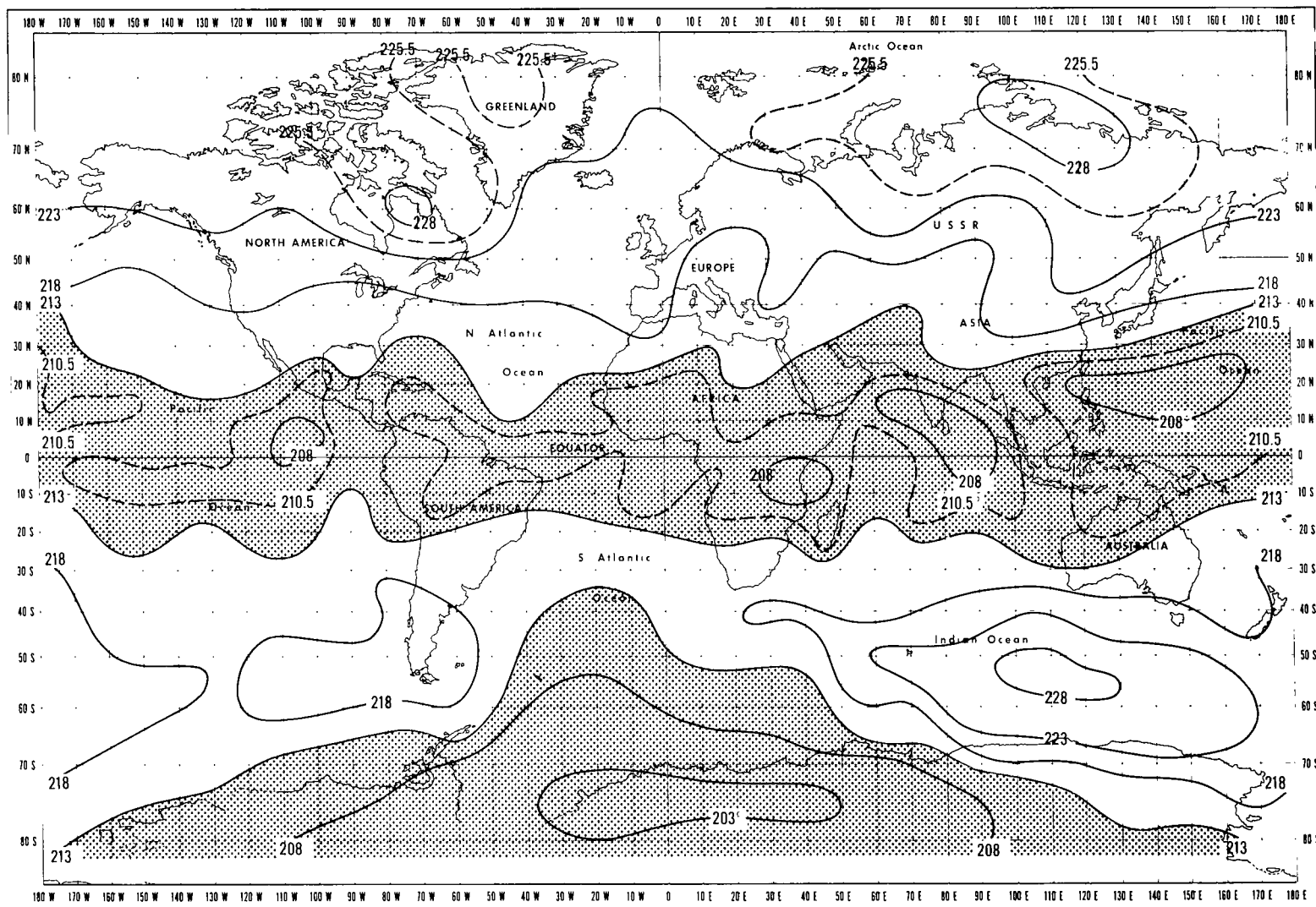Figure A-4(b)—10-mb temperatures (K), Nimbus 3 IRIS data, April 28, 1969.

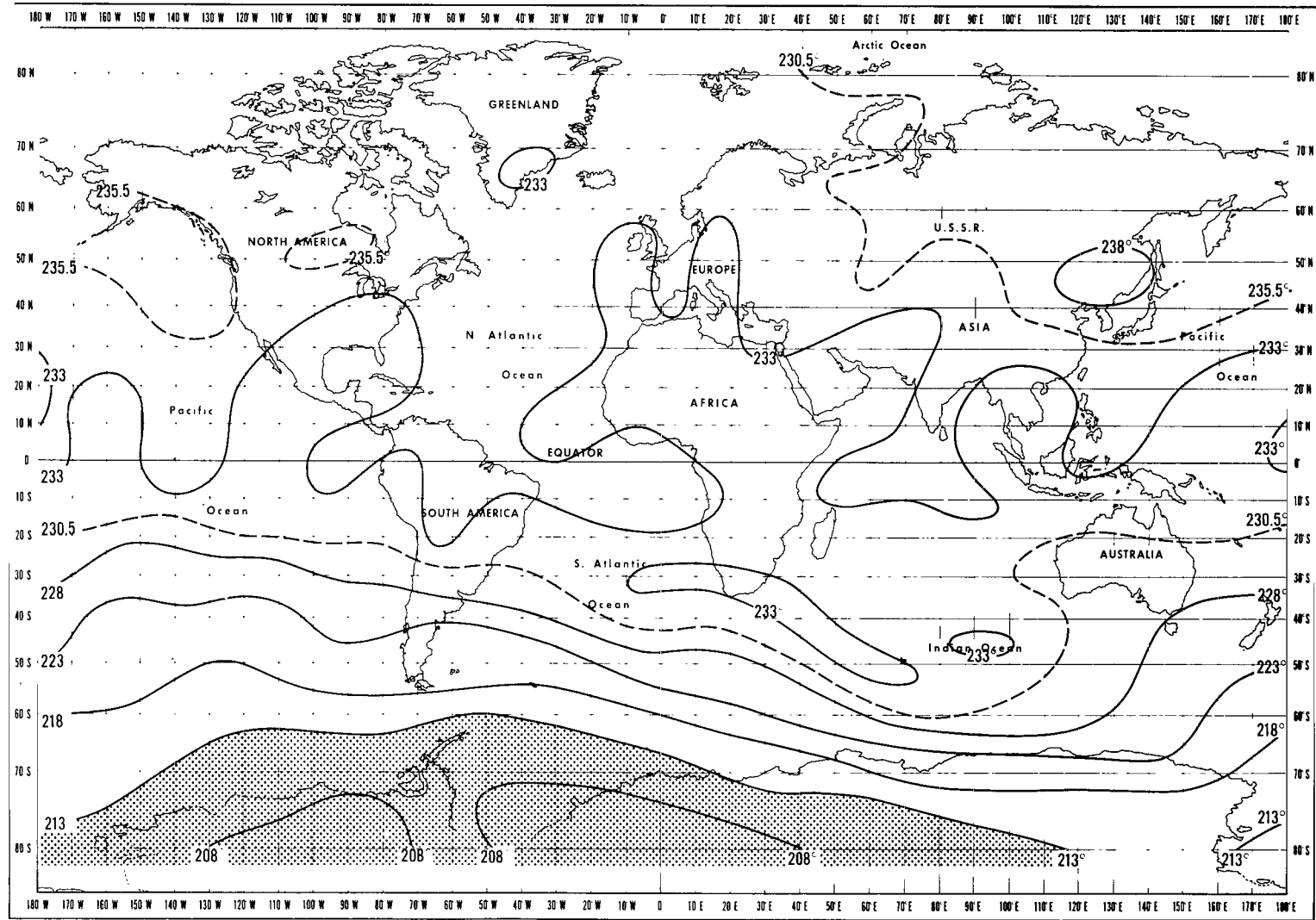Figure A-5(a)—50-mb temperatures (K), Nimbus 3 IRIS data, April 29, 1969.

Figure A-5(b)—10-mb temperatures (K), Nimbus 3 IRIS data, April 29, 1969.

"The aeronautical and space activities of the United States shall be conducted so as to contribute ... to the expansion of human knowledge of phenomena in the atmosphere and space. The Administration shall provide for the widest practicable and appropriate dissemination of information concerning its activities and the results thereof."

— NATIONAL AERONAUTICS AND SPACE ACT OF 1958

NASA SCIENTIFIC AND TECHNICAL PUBLICATIONS

TECHNICAL REPORTS: Scientific and technical information considered important, complete, and a lasting contribution to existing knowledge.

TECHNICAL NOTES: Information less broad in scope but nevertheless of importance as a contribution to existing knowledge.

TECHNICAL MEMORANDUMS: Information receiving limited distribution because of preliminary data, security classification, or other reasons.

CONTRACTOR REPORTS: Scientific and technical information generated under a NASA contract or grant and considered an important contribution to existing knowledge.

TECHNICAL TRANSLATIONS: Information published in a foreign language considered to merit NASA distribution in English.

SPECIAL PUBLICATIONS: Information derived from or of value to NASA activities. Publications include conference proceedings, monographs, data compilations, handbooks, sourcebooks, and special bibliographies.

TECHNOLOGY UTILIZATION PUBLICATIONS: Information on technology used by NASA that may be of particular interest in commercial and other non-aerospace applications. Publications include Tech Briefs, Technology Utilization Reports and Technology Surveys.

Details on the availability of these publications may be obtained from:

SCIENTIFIC AND TECHNICAL INFORMATION OFFICE

NATIONAL AERONAUTICS AND SPACE ADMINISTRATION
Washington, D.C. 20546